Abundant *trans*-driven variation in detoxification gene expression in the extreme generalist herbivore *Tetranychus urticae*

Andre H Kurlovs[1,2¶], Berdien De Beer[1¶], Meiyuan Ji[2¶], Marilou Vandenhole[1], Tim De Meyer[3], René Feyereisen[1,4], Richard M Clark[2,5*], Thomas Van Leeuwen[1*]

[1] Department of Plants and Crops, Faculty of Bioscience Engineering, Ghent University, Ghent, Belgium

[2] School of Biological Sciences, University of Utah, Salt Lake City, United States of America

[3] Department of Data Analysis and Mathematical Modelling, Faculty of Bioscience Engineering, Ghent University, Ghent, Belgium

[4] Department of Plant and Environmental Sciences, University of Copenhagen, Thorvaldsensvej, Copenhagen, Denmark

[5] Henry Eyring Center for Cell and Genome Science, University of Utah, Salt Lake City, United States of America

*Corresponding authors

E-mail: clark@biology.utah.edu (RMC); Thomas.VanLeeuwen@UGent.be (TVL)

¶ These authors contributed equally to this work.

Short title: Gene expression regulation in *Tetranychus urticae*

Abstract

The extreme adaptation potential of the generalist herbivore *Tetranychus urticae* (the two-spotted spider mite) to pesticides as well as diverse host plants has been associated with clade-specific gene expansions in known detoxifying enzyme families, and with extensive and rapid transcriptional responses. However, how this broad transcriptional potential is regulated remains largely unknown. Using a parental/F1 design in which four inbred strains were crossed to a common inbred strain, we assessed the genetic basis and inheritance of gene expression variation in *T. urticae*. Mirroring known phenotypic variation in the progenitor strains of the inbreds, we confirmed that the inbred strains we created were genetically distinct, varied markedly in pesticide resistance, and also captured variation in host plant fitness commonly observed in this species. By examining differences in gene expression between parents and allele-specific expression in F1s, we found that variation in RNA abundance was more often explained in *trans* as compared to *cis*, with the former associated with dominance in inheritance. Strikingly, in a gene ontology analysis, detoxification genes of the cytochrome P450 monooxygenase (CYP) family, as well as dioxygenases (DOGs) acquired from horizontal gene transfer from fungi, were specifically enriched at the extremes of *trans*-driven up- and downregulation. In particular, a clade of CYPs with documented broad substrate-specificity including multiple pesticides, as well as DOGs that have recently been shown to have broad substrate specificity against plant specialized compounds, were exceptionally highly upregulated as a result of *trans* effects (or in some cases synergism of *cis* and *trans*) in the most multi-pesticide resistant strains. Collectively, our findings highlight the potential importance of *trans*-driven expression variation in genes associated with xenobiotic metabolism and host plant use for rapid adaptation in *T. urticae*, and also suggest modular control of these genes, a regulatory architecture that might ameliorate negative pleiotropic effects.

Author summary

The two-spotted spider mite, *Tetranychus urticae,* is a generalist herbivore and pest of diverse crops globally. In response to the plethora of chemicals used for its control, the species rapidly evolves pesticide

resistance. Further, experimental evolution studies with *T. urticae* populations have demonstrated adaptation to challenging host plants in as few as five generations. The adaptation of *T. urticae* to pesticides and host plants has been associated with large transcriptome changes, including for genes associated with detoxification of pesticides and toxic plant compounds. Nevertheless, the basis of the observed transcriptome variation has remained largely unknown. Here, we examined the genetic control and inheritance of expression differences among five inbred *T. urticae* strains, including several with histories of intense pesticide selection. With a parental/F1 experimental design, we found that *trans* effects were common in explaining variation in detoxification gene expression, with the *trans*-driven upregulation of a subset of cytochrome P450 monooxygenases of broad substrate specificity especially striking in the most pesticide resistant strains. Our findings suggest that genetic variation acting with dominant or additive inheritance to impact the regulation of modules of detoxification genes may be an important target of selection during rapid pesticide and host plant evolution in herbivores.

71 # Introduction

72 Genetic variation as a requisite for evolutionary change through selection, recombination and drift lies at
73 the basis of our current understanding of evolution [1,2]. Nucleotide changes in coding sequences were
74 among the first to be associated with phenotypic differences of adaptive significance. Subsequently,
75 advances in genomic methods have facilitated a broader understanding of how other types of coding
76 sequence variation – such as structural or copy number variation – impact phenotypes [3,4]. Likewise, a
77 number of specific instances of regulatory variation in genic regions impacting gene expression phenotypes
78 of adaptive relevance have been characterized in detail [5–8]. More recently, advances in experimental
79 designs and methods have allowed the genetic control of gene expression variation to be assessed genome-
80 wide [9,10], offering the possibility of a more comprehensive understanding of how such variation arises
81 and is selected upon to impact phenotypes [11].

82 One widely used approach to understand the genetic control of gene expression variation, as well
83 as its associated inheritance, involves comparing expression between parents and F1 offspring [9,12–21].
84 If a difference in gene expression between two individuals or parental strains is due to *cis* effects only (i.e.,
85 changes in promoter or enhancer regions), the same difference in expression will be observed between the
86 respective parental allele copies in F1 offspring (i.e., allele-specific expression, or ASE). However, if
87 expression differences between parents are not observed in F1 ASE (or parental and ASE patterns contrast),
88 *trans* effects contribute to regulatory variation [9]. This type of parental/F1 design also enables the degree
89 of dominance – an important factor in understanding responses to selection – to be inferred [14,19–21]. A
90 number of studies in diploid organisms, often using genetic models selected in part because of their
91 extensive genomic resources, have revealed trends about the frequency of *cis* and *trans* effects, their
92 interactions, as well as associations with inheritance type. For example, in many instances, expression
93 variation more often results from *trans* versus *cis* regulation in intraspecific comparisons, with the opposite
94 pattern observed for interspecific ones ([22], and references therein). Further, while *trans* regulation is

95 associated with dominance or non-additivity in gene expression inheritance, genes with *cis* effects are
96 enriched for additive inheritance [14,16,19–21].

97 However, despite the resolution and comprehensive nature of parental/F1 and related experimental
98 designs, connecting the genetic variation that impacts gene expression to adaptation has remained
99 challenging. In part, this results from a lack of understanding of underlying selective forces. A classic
100 example of rapid adaptation for which the agent(s) are known explicitly is pesticide resistance evolution.
101 This phenotype has been studied extensively in arthropods, including in herbivores [23–26]. For the
102 herbivorous insects and mites that consume plant tissue, chemical control by pesticides is widely used.
103 Resistance evolution is a major obstacle for agriculture, and understanding inheritance (dominance or lack
104 thereof) can be critical to inform approaches for resistance management [27–29]. Further, albeit with less
105 precision in space, time, or nature of the selective agent(s), adaptation of herbivores to their host plants has
106 also provided well-known examples of evolution in action [30–34]. Finally, a number of gene families have
107 been associated with the detoxification, sequestration, or transport and excretion of pesticides, and are either
108 known or are likely to be critical in plant host adaptation as well (i.e., to overcome toxic plant-produced
109 specialized compounds, although plants deploy other defense strategies as well) [33–41]. Therefore, many
110 selective agents are known for adaptation in herbivores, sometimes exactly (pesticides), as are genes and
111 gene families that are strong candidates to underlie rapid phenotypic evolution.

112 In this study, we have determined the genetic basis and inheritance of gene expression variation
113 among strains of the two-spotted spider mite, *Tetranychus urticae*. This generalist (polyphagous) mite is at
114 the extreme end of the generalist-to-specialist spectrum, as it has been documented to feed on a staggering
115 1,100 plant species from more than 250 plant families, including more than 150 crops [42]. In addition, *T.*
116 *urticae* is well known for developing acaricide resistance in as fast as a few years after the introduction of
117 most acaricides used for its control (acaricides are pesticides that are active against mites, which belong to
118 the Acari within Arthropoda subphylum Chelicerata) [25]. The extreme adaptation potential of this species
119 has been associated with clade-specific gene expansions in known detoxifying enzyme families, such as
120 cytochrome P450 monooxygenases (CYPs), mu-class glutathione-S-transferases (GSTs), a new clade of

121 carboxyl-choline esterases (CCEs), and an unexpectedly large repertoire of ATP-binding cassette (ABC)
122 and major facilitator superfamily (MFS) transporters [33,36,42]. In addition, it acquired several putative
123 detoxification genes by horizontal gene transfer that subsequently proliferated in the genome [43]. These
124 include intradiol-ring cleavage dioxygenases (DOGs) that have recently been shown to cleave an
125 unexpectedly wide range of aromatic plant defense specialized compounds [41], as well as bacterial UDP-
126 glucuronosyltransferases (UGTs) [44], demonstrating the adaptive advantage of horizontal gene transfer in
127 the context of detoxification and host plant use [42,43,45]. Gene-expression studies have revealed large and
128 similar transcriptomic differences in these gene families between acaricide susceptible and resistant *T.*
129 *urticae* strains, as well as after adaptation to new host plants [33,34,46], suggesting a link between host
130 plant use and acaricide resistance. The extensive and rapid transcriptional reprogramming associated with
131 the exceptional adaptation potential of *T. urticae* raises several questions about the mechanisms of gene
132 regulation in polyphagous herbivores. Given the often very large population sizes of this species in
133 agricultural settings, selection acting on *cis* variants at many loci is plausible. However, the often
134 coordinated and rapid responses in gene expression patterns observed between strains after selection by
135 both acaricides and host plants [33,34] raises the alternative possibility of selection acting on *trans*-acting
136 factors that serve as master regulators of detoxification/adaptation pathways.

137 As opposed to many herbivores, *T. urticae* has a short life cycle and a high-quality genome, and is
138 easy to inbreed [47]. Therefore, it is optimally suited for a study relying on F1s from parental strain crosses
139 to determine *cis*/*trans* contributions to and inheritance of gene expression. Here, we selected four
140 genetically divergent *T. urticae* strains with different evolutionary histories, including two highly multi-
141 acaricide resistant strains, and inbred them. We then crossed the inbred strains to a common inbred parental
142 strain that was comparatively susceptible to most acaricides tested. Using parental/F1 experimental designs,
143 we observed extensive expression differences among strains. We found that gene expression differences
144 arising from *trans* variation were common, including for subsets of genes in multiple detoxification gene
145 families, indicative of modular control of detoxification and plant host associated pathways in this generalist

146 mite pest. Notably, *trans* control contributed prominently to the exceptionally high expression of a clade of
147 CYPs with broad substrate specificity in the acaricide resistant strains.
148

149 Results

150 Five inbred strains harbor extensive genetic variation

151 Strains of *T. urticae* used in this study were selected based on their different life histories and acaricide
152 resistance status (see Methods). Briefly, strains MR-VP and MAR-AB originated from European strains
153 previously found to be multi-acaricide resistant [33,48], strain JP-RR originated from a Japanese strain
154 resistant to several classes of mitochondrial electron transport inhibitors (METI) [49], while strain ROS-IT
155 was recently collected in Italy and was highly resistant to abamectin [50]. Finally, strain SOL-BE originated
156 from a Belgian potato field which had not undergone any acaricide treatment. To fix intra-population
157 genetic variation, a prerequisite for our downstream analyses, each of the five strains was inbred by mother-
158 son crossings for at least seven generations. The subsequent inbred strains, denoted MR-VPi, MAR-ABi,
159 JP-RRi, ROS-ITi, and SOL-BEi, were used for all subsequent analyses, including genome sequencing.
160 Resulting Illumina DNA-seq reads for each strain were aligned to the ~90 Mb *T. urticae* three-chromosome
161 reference assembly [51], and median coverages ranged from 98- (MAR-ABi) to 430-fold (ROS-ITi).
162 Among the five strains, variant prediction revealed 1.19 million high-quality variants (SNPs and small
163 indels), consistent with prior studies that have revealed substantial variation among *T. urticae* strains [51–
164 54]. Further, more than 98% of SNP sites were fixed in each of the five strains, confirming earlier reports
165 that ~7 generations of inbreeding in this haplodiploid species results in isogenic (or nearly isogenic) strains
166 [52]. To assess genetic relationships among strains, we performed a principal component analysis (PCA)
167 using the SNP data (Fig 1A). While the inbreeding of the five strains was performed as part of the current
168 study, the SOL-BEi and MAR-ABi strains, and respective genomic sequence and parental RNA-seq data
169 generated for these strains, was used by De Beer et al. [55] in a bulk segregant analysis (BSA) study that
170 identified two quantitative trait loci (QTL) for resistance to the acaricide fenbutatin oxide [55]. Our PCA

171 using all strains confirmed De Beer et al.'s [55] observation that SOL-BEi and MAR-ABi are genetically
172 distinct, and moreover we found that SOL-BEi was highly divergent from each of the other three inbred
173 strains. Two strains, MR-VPi and JP-RRi, did cluster nearby each other in the PCA analysis, but were
174 nevertheless distinct along both PC axes 1 and 2, which explained 29.9% and 25.1% of the variance in this
175 analysis, respectively.
176

177 The inbred strains have diverse and contrasting resistance profiles

178 In *T. urticae*, high levels of acaricide resistance and histories of exposure are often associated with variation
179 in expression of genes encoding detoxification enzymes and transporters. To assess whether the inbred
180 strains vary in acaricide resistance and life histories, we evaluated their levels of resistance to 12 acaricides
181 belonging to multiple classes (Fig 2A and S1 Table), and also determined their distribution of target-site
182 resistance mutations (Fig 2A and S2 Table). The five strains were distinguishable in their resistance to most
183 acaricide classes, although fewer differences were observed for the METI-II and METI-III compounds.
184 Across classes, several trends stood out. MR-VPi and MAR-ABi, for which progenitor populations were
185 previously reported to be multi-acaricide resistant, exhibited the highest levels of resistance to compounds
186 in multiple acaricide classes (Fig 2A). This was especially true for Na^+ channel modulators, GluCl allosteric
187 modulators, inhibitors of mitochondrial ATP synthase, and METI-I compounds. Compared to MR-VPi,
188 which is notably more resistant to METI-Is, MAR-ABi exhibited higher resistance to other classes,
189 especially for inhibitors of mitochondrial ATP synthase (this study and De Beer et al. [55]). In contrast to
190 MR-VPi and MAR-ABi, JP-RRi showed intermediate resistance to most acaricide classes, with modestly
191 higher resistance levels to METI-II compounds. While the resistance profile of SOL-BEi was similar to JP-
192 RRi, it was more resistant to the Na^+ channel modulator bifenthrin. Unexpectedly, although ROS-ITi
193 showed high susceptibility to most compounds tested, its level of resistance to dicofol (unknown target)
194 was the highest among all strains (Fig 2A).

195 To further test for life histories that include exposure to acaricides, we used the genomic sequencing
196 data and variant calls (Fig 1A) to survey target-site resistance mutations across strains (Fig 2A). Resistance
197 to dicofol is poorly understood. However, target-site mutations that confer resistance to the other acaricides
198 used in this study have been identified (S2 Table). Both MR-VPi and MAR-ABi have the resistance-
199 conferring H110R mutation in METI-Is' target gene *PSST* (*tetur07g05240*) [52,56]. ROS-ITi and MAR-
200 ABi have the two synergistic resistance mutations in the glutamate-gated chloride channel, G314D and
201 G314E in *GluCl1* (*tetur02g04080*) and *GluCl3* (*tetur10g03090*), respectively, and are resistant to the
202 glutamate channel inhibitor abamectin [57]. The L915M mutation in the voltage gated sodium channel
203 (*VGSC*, *tetur34g00970*) is associated with resistance to pyrethroids in *Varroa destructor* [58–60], and was
204 present in all the strains highly resistant to bifenthrin (SOL-BEi, MAR-ABi, and MR-VPi). Further, a recent
205 BSA study that used two sets of fenbutatin oxide susceptible and resistant parental strains, including SOL-
206 BEi and MAR-ABi, identified a candidate target site resistance mutation (V89A) for fenbutatin oxide in
207 the gene encoding subunit c of *mitochondrial ATP-synthase* (*tetur06g03780*) (present in resistant MAR-
208 ABi, absent in susceptible SOL-BEi) [55]. We also found this mutation in ROS-ITi in addition to MAR-
209 ABi; however, as noted by De Beer et al. [55], this gene is duplicated and while the parental MAR-AB
210 outbred strain was reported to have the mutations in both copies, only a single copy bears the mutation after
211 inbreeding in both MAR-ABi and ROS-ITi. This probably explains the absence of resistance in ROS-ITi,
212 and strongly suggests additional metabolic mechanisms of resistance in MAR-ABi. Indeed, and more
213 generally, although the overall presence of target-site resistance mutations is consistent with previous
214 acaricide exposure and can be used as bio-markers [61,62], they nevertheless are not the only determinants
215 of resistance, as multiple studies have now shown [51–53,63]. This is also clear from the data in this study,
216 as resistance ratios varied markedly even among strains with the same target-site resistance mutation (e.g.,
217 between MR-VPi and MAR-ABi for two of three METI-I compounds, or between MAR-ABi and ROS-ITi
218 for abamectin), and thus other resistance mechanisms are almost certainly involved (see Discussion).
219 Finally, although we did not assess resistance of strains to the widely used mite growth inhibitors

220 hexythiazox, clofentezine, and etoxazole, each of the five strains harbored the I1017F target-site variant in
221 *chitin synthase 1* (*CHS-1*, *tetur03g08510*) that confers resistance to these three compounds [64,65].
222

223 **Fitness on different host plants**

224 We also used fecundity as a proxy for evaluating the performance of four of the inbred strains (ROS-ITi,
225 JP-RRi, MAR-ABi and MR-VPi) on five host plant species known to vary greatly in their production of
226 specialized compounds, as well as other anti-herbivore defenses [39,66]. These included bean (*Phaseolus*
227 *vulgaris*), a favorable host widely used for the propagation of laboratory strains of *T. urticae*, as well as
228 tomato (*Solanum lycopersicum*), cucumber (*Cucumis sativus*), prune (*Prunus domestica*) and potato
229 (*Solanum tuberosum*). As shown in Fig 2B, the fecundity (as measured by eggs laid) of female mites was
230 higher on bean, cucumber, and prune than on tomato and potato, which belonged to the family Solanaceae.
231 Interestingly, while ROS-ITi performed statistically worse on bean, cucumber, tomato and potato than one
232 or more of the other strains, this pattern was not apparent on prune (ANOVA, with post-hoc t-tests with
233 Tukey corrections for multiple testing, p-values < 0.05). In contrast, JP-RRi showed significantly higher
234 reproductivity on bean, cucumber, prune and potato as compared to one or more other strains. However, it
235 had significantly lower fecundity on tomato than MAR-ABi, with very few eggs laid. MAR-ABi and MR-
236 VPi, which showed the most pronounced multi-acaricide resistance (Fig 2A), did not stand out from other
237 strains on their performance on most hosts. However, on tomato, both MAR-ABi and MR-VPi had higher
238 fecundity than other strains (although only MAR-ABi had significantly higher fecundity than ROS-ITi and
239 JP-RRi). Collectively, our results demonstrate that we captured genetic variation among strains impacting
240 fitness on different host plants.
241

242 **Variation in gene expression in inbred strains associates imperfectly with**

243 **genetic distance**

244 Prior transcriptomic studies using strains of *T. urticae* susceptible or resistant to specific acaricides have
245 identified over-expression of detoxification genes in several families as potentially causal for resistance
246 phenotypes [33,53,67–69]. Further, studies using the parental (outbred) populations of MAR-ABi and MR-
247 VPi revealed large differences in the expression of genes in most known detoxification gene families, as
248 well as for many other genes, as compared to the acaricide susceptible London reference strain [33,36].
249 However, the outbred nature of these strains, coupled with the lack of F1 data, precluded assessment of the
250 regulatory modes for gene expression variation at a genome-wide scale.

251 To understand the genetic control and inheritance of gene expression variation between *T. urticae*
252 strains that vary in acaricide resistance and host performance, we collected RNA-seq data for each of the
253 five inbred strains included in our study, as well as F1 data from crosses of each of ROS-ITi, JP-RRi, MAR-
254 ABi, and MR-VPi to the SOL-BEi strain. Briefly, SOL-BEi was selected as the common parent in each of
255 the crosses because it was genetically distinct from the other strains (Fig 1A), it was comparatively acaricide
256 sensitive (Fig 2A), and because test crosses revealed that viable F1 progeny were readily produced for each
257 of the four crosses (genetic incompatibilities or partial incompatibilities are not uncommon among *T.*
258 *urticae* strains [54,70–72]). RNA was collected from 4-7-day old adult females on a single host plant (bean)
259 with either four or five biological replicates for parental strains and resulting F1s (Fig 1B). To assess gene
260 expression variation among genotypes, resulting RNA-seq reads were aligned to the three chromosome
261 London reference genome assembly [51]. To reduce the impact of intra-specific DNA variation among
262 strains on read alignments, genetic variants - identified from genome sequencing and variant prediction
263 (Fig 1A) for each of the five strains - were provided to GSNAP, a variant-aware RNA-seq read mapper (see
264 Methods) [73,74]. A PCA based on transcriptome data revealed that replicates for each strain clustered
265 together and away from other strains, and that F1s had approximately intermediate transcriptomic patterns
266 between each set of parents. While the relative pattern of clustering of parental expression replicates was

267 broadly similar to that observed for genetic variant data, in the PCA based on expression data JP-RRi
268 clustered more closely to MAR-ABi, and further away from MR-VPi, than observed with genetic data
269 (compare Fig 1B to Fig 1A).
270

271 Prominent *trans* control of expression variation among inbred strains

272 In experimental designs with parental inbred strains (parents) and F1s, the comparison of expression
273 differences between parents, and of ASE in the F1s, allows detection and assignment of regulatory modes
274 underlying gene expression variation. For subsequent analyses, in pairwise comparisons – the crosses of
275 ROS-ITi, JP-RRi, MAR-ABi, and MR-VPi to the SOL-BEi, and the respective F1s – we assessed the
276 genetic mode of control for genes with polymorphisms (SNPs) in exons, a requirement for the measurement
277 of ASE (given variable annotation of untranslated regions in the *T. urticae* genome, we restricted our
278 analyses to coding exons). For consideration for inclusion in a given comparison, we also required genes
279 to be putatively intact in each of the two strains (i.e., no obvious disrupting sequence differences like
280 premature stop codons as assessed from variant predictions), and to have no evidence of copy number
281 variation as assessed with DNA-seq read depth. For these and other criteria used for the selection of the
282 intact+single copy gene sets, including the use of RNA-seq data to further identify potential copy variable
283 genes, see the Methods. Applying these criteria, the resulting numbers of genes for which assignment of
284 genetic mode of control could be attempted ranged from 8,232 in the JP-RRi × SOL-BEi comparison
285 (43.1% of the total 19,087 annotated protein coding genes) to 8,880 in the MR-VPi × SOL-BEi comparison
286 (46.5%); 4,921 genes (25.8%) could be analyzed in all four of the crosses (S1 Fig and S3 Table). The total
287 number of genes, 19,087 in the ~90 Mb *T. urticae* genome, includes many small, hypothetical predictions
288 that were retained in the annotation, a potentially contributing factor to the modest percent of genes included
289 in the analysis (e.g., these sequences may not be functional and therefore conserved). In F1 samples for
290 intact+single copy genes for which SNPs were present, we recovered and quantified parent-of-origin reads,
291 and quantified reads from the respective parental replicates at the same sites using the same workflow.

292 By performing differential gene expression analyses between parental strains, and ASE
293 identification in F1s, we determined differential gene expression and assigned modes of control (adjusted
294 $p < 0.1$). After McManus et al. [14], genes showing differential expression either between parents and/or
295 ASE in F1s were sorted into five main categories of control: (1) *cis* effects only (hereafter *cis*), (2) *trans*
296 effects only (hereafter *trans*), (3) synergism, where *cis* and *trans* act in the same direction with respect to
297 one parent (in our case, ROS-ITi, JP-RRi, MAR-ABi, and MR-VPi as compared to SOL-BEi), (4)
298 antagonism, where *cis* and *trans* act in opposite directions with respect to one of the parents, and (5)
299 compensatory, where there is significant ASE but no differential expression between the parents, a result
300 of offsetting *cis* and *trans* effects (a special case of antagonism). Genes showing no differential expression
301 between parental strains and no ASE differences in F1s were classified into a sixth category, conserved.
302 Genes that could not be assigned into any of these six categories because of conflicts between criteria for
303 classification were assigned as ambiguous (further, no attempt at assignment was made for genes with no
304 or low expression, see Methods). In total, genetic mode of control assignments for these categories could
305 be made for between 5,630 (the ROS-ITi × SOL-BEi comparison) to 5,847 (the MAR-ABi × SOL-BEi
306 comparison) of intact+single copy genes (S1 Fig and S4 Table). For 3,381 genes, assignments could be
307 made across all four comparisons.

308 Across the four comparisons, between 51.9% to 66.4% of genes fell into the *cis*, *trans*, synergism,
309 antagonism, or compensatory categories, with the majority of the remaining genes having conserved
310 expression (S2 Fig and S4 Table). Among all genes for which a genetic mode of control - *cis*, *trans*,
311 synergism, antagonism, or compensatory - could be assigned, those with *trans* control were more numerous
312 by between 2.80- to 3.23-fold as compared to the second most frequent category (*cis*), excepting for the
313 ROS-ITi × SOL-BEi comparison (1.69-fold, Fig 3A-D). However, with increasing magnitude of $\log_2$ fold
314 change ($\log_2$FC) between parents, the relative number of genes classified as regulated in *trans* decreased
315 markedly relative to those regulated in *cis* (e.g., from ~51.4% to ~16.4% across comparisons in bins of
316 absolute value of parental $\log_2$FC of < 1 to $\log_2$FC >2, while the fraction of genes with *cis* control increased
317 from ~18.1% to ~32.1%, Fig 4A). Further, as fold change increased, genes in the synergism category

318 increased dramatically, an expected finding (i.e., conditioning on increasing fold change enriches for
319 synergism because the two modes of control, *cis* and *trans*, contribute in the same direction to parental fold
320 change). As shown in Fig 3A-D, and in Fig 4A, comparatively little difference in these trends was observed
321 between crosses when considering all genes, apart from the relatively high percent of *cis* control in the
322 lower fold change categories in the ROS-ITi × SOL-BEi comparison (Fig 4A).
323

324 Patterns of genetic control for genes associated with xenobiotic resistance and 325 host plant use

326 Given the phenotypic differences in resistance and host performance among the inbred strains, we examined
327 more specifically differential gene expression and its genetic control for genes in families implicated in the
328 metabolism, transport, and binding of acaricides and plant defense compounds (detoxification gene set, D,
329 723 genes), host plant use (host genes, H, 318 genes), and a subset of mite peptidases that are potentially
330 involved in overcoming plant produced anti-herbivore protease inhibitors (peptidase gene set, P, 58 genes)
331 (the combined "D+H+P" gene set has 1069 genes; S5 Table). The selection of the detoxification and
332 peptidase gene families and genes are described in the Methods; briefly, the host gene set consists of genes
333 that were previously associated with adaptation of the reference *T. urticae* strain London to tomato as a new
334 host, most of which currently have an unknown function [34] (host genes with overlap to the detoxification
335 gene set were removed from the host genes set, resulting in 288 genes).

336 Between 32.3-33.2% of genes in the D+H+P gene set were included in our analyses across the four
337 comparisons, a modestly higher fraction than for all genes (29.5-30.6%). As compared to all genes,
338 relatively fewer D+H+P genes fell into the *cis* category in most comparisons, although samples sizes for
339 D+H+P genes were modest, especially following stratification by the absolute value of $\log_2$FC between
340 parents (compare Fig 4A to Fig 4B). Despite the comparatively small sample sizes, however, a greater
341 relative proportion of D+H+P genes were present in categories of higher absolute value of $\log_2$FC between
342 parents than for the background sets of all genes in each comparison (contrast subpanels between Fig 4A

343 and Fig 4B for each of the four comparisons; all *p*-values for chi-square tests between all genes and D+H+P
344 genes were < 10^{-5}). Further, among the D+H+P genes with an absolute value $\log_2$FC > 1 (between parents,
345 or for ASE in F1s), genes in nearly all detoxification gene families, as well as peptidases, were present in
346 each comparison, including a substantial fraction of genes encoding DOGs, lipocalins, and UGTs in one or
347 more comparison (Fig 3E-H). Overall, host genes followed a broadly similar pattern as for the detoxification
348 gene set. Finally, many genes at the extremes of differential expression magnitude belonged to the D+H+P
349 set (compare Fig 3E-H to Fig3A-B), including both up- and downregulated genes (e.g., for genes with an
350 absolute value $\log_2$FC of greater than four, especially for the comparisons of JP-RRi, MAR-ABi, and MR-
351 VPi to SOL-BEi, Fig 3B vs. Fig 3F, Fig 3C vs. Fig 3G, and Fig 3D vs. Fig 3H, respectively).
352

353 CYPs linked to metabolism of known acaricides are among the genes with
354 strongest *trans* regulation

355 The analyses presented in Fig 3 and Fig 4 revealed that many genes in the D+H+P set exhibited strong
356 differential expression, with many controlled in *trans,* some in *cis*, and many with a combination of both.
357 In a complementary approach independent of *a priori* gene family classification, we also investigated the
358 molecular nature of genes with high differential expression as a function of their genetic control mode. To
359 do this, we performed a gene ontology (GO) enrichment analysis (molecular function, MF) on genes
360 showing extremes in fold changes between parents conditioned on contributions of *cis* or *trans* regulation;
361 in this analysis, information across the four comparisons was combined (see Methods), and the top 2.5% of
362 genes in the up- or downregulated tails of the respective distributions were assessed. Strikingly, no GO
363 terms were significantly enriched when considering *cis* for either up- or downregulation (adjusted $p < 0.05$).
364 However, two GO terms were significantly enriched for *trans*-driven upregulation – GO:0005506 ("iron
365 ion binding") and GO:0016491 ("oxidoreductase activity") (S6 Table). GO:0005506 included eight CYPs
366 and four DOGs. The term GO:0016491 primarily consisted of short-chain dehydrogenases/reductases
367 (SDRs), but also included six other genes, including ones encoding a sorbitol dehydrogenase

368 (*tetur04g07030*) and a phytoene dehydrogenase (*tetur11g04820*). In addition, GO:0005506 ("iron ion
369 binding") was enriched among genes showing high levels of *trans*-driven downregulation, and included six
370 CYPs, three DOGs, and a gene encoding an oxoglutarate/iron-dependent oxygenase (*tetur20g01680*) (S6
371 Table).

372 The striking finding of this analysis was that many genes contributing to the *trans* enriched GO
373 terms were already in the detoxification gene set, especially CYPs. Because of this, and because CYPs are
374 important players in detoxification in *T. urticae* and across the animal kingdom [37], we examined more
375 closely the patterns of differential expression and *cis*/*trans* regulation within this gene family (Fig 5). We
376 found that of the eight CYPs enriched for extremes of *trans*-control in the GO analysis (upregulation relative
377 to SOL-BEi, GO:0005506), five belonged to the CYP392 family (Fig 5, CYP2 clan) that has previously
378 been implicated in acaricide detoxification (see Discussion). As compared to SOL-BEi, the most striking
379 upregulation of these genes was observed in the multi-acaricide resistant strains MAR-ABi and MR-VPi,
380 and the least dramatic changes were observed for ROS-ITi, which is comparatively acaricide sensitive. This
381 was particularly striking for the closely related *CYP392A11, CYP392A12,* and *CYP392A16* genes, for which
382 strong upregulation was explained predominantly in *trans*. However, *trans*-driven upregulation was not
383 universal for CYP392 family members, as both *CYP392B1* and *CYP392B3* exhibited downregulation
384 resulting from *trans* effects in MAR-ABi and MR-VPi (and for *CYP392B3*, in other strain contrasts as
385 well). For only a few CYP392 genes did *cis* effects contribute substantially to the overall direction of
386 differential expression between parents (i.e., the upregulation of *CYP392E2* in JP-RRi, or the upregulation
387 of *CYP392D1* in all strains). In many cases, synergism or antagonism were observed, and *cis* effects, albeit
388 relatively minor, contributed synergistically to the very high expression levels of *CYP392A11, CYP392A12*
389 and *CYP392A16* in most strains as compared to SOL-BEi.

390 In addition to CYP392 genes from the CYP2 clan, *trans*-driven upregulation was also observed for
391 *CYP385A1* and *CYP385B1* from the CYP3 clan and *CYP389B1* from the CYP4 clan, and in general a trend
392 for *trans*-driven upregulation of CYP385 genes was observed, particularly in the comparison with ROS-ITi
393 (although $\log_2$FC values were low to modest as compared to some CYP392 genes). Further evidence that

394 related CYP genes can show divergent expression control in *trans* is provided by three CYP389 genes in
395 CYP4 clan with high levels of *trans* control, in which the direction of the *trans* effect was up for *CYP389B1*
396 (for strain MAR-ABi), and down for *CYP389C1* (for strains MAR-ABi and MR-VPi) and *CYP389C11* (for
397 strains JP-RRi, MAR-ABi and MR-VPi).

398 Although we focused on CYPs, similar patterns were observed for other detoxification genes. For
399 instance, the most striking differences in expression between parents was often explained primarily by *trans*
400 effects, as observed for the DOG genes *DOG1*, *DOG11*, and *DOG13* (in MAR-ABi) (S3 Fig), the lipocalins
401 *tetur24g01030*, *tetur01g05740*, and *tetur01g05730* (in MAR-ABi or MR-VPi) (S4 Fig), or the SDRs
402 *tetur06g05090* (in ROS-ITi and JP-RRi) and *tetur06g04970* (in JP-RRi, MAR-ABi, and MR-VPi) (S5 Fig).
403 Further, as seen for the CYP genes, evidence for regulatory complexity among genotypic comparisons for
404 other detoxification genes was readily apparent (S3-S5 Figs and S4 Table). Examples include the lipocalin
405 gene *tetur01g05740*, which was upregulated in both MAR-ABi and JP-RRi as compared to SOL-BEi, with
406 the former explained predominantly by a *trans* effect, while for the latter only a *cis* effect was predicted. In
407 contrast, for the lipocalin gene *tetur04g06010*, *trans* control contributed to large expression differences in
408 MAR-ABi and MR-VPi as compared to SOL-BEi, but in contrasting directions (up in MAR-ABi, down in
409 MR-VPi), reflecting the opposing parental expression differences.

410

411 **Dominant inheritance is common for genes controlled in *trans***

412 In addition to allowing the determination of genetic modes of gene expression control, the parental/F1
413 experimental design also allowed assignment of expression inheritance, which we assessed by using total
414 read counts for all intact+single copy genes (S3 Table) (note that the determination of inheritance does not
415 rely on ASE). Gene expression inheritance was assigned using the following categories: additive (when F1
416 expression equals the intermediate expression of parents), dominant (when F1 expression equals the level
417 of either one of the two parents) and transgressive (when F1 expression falls outside the range of both
418 parents) [20]. Using strict criteria, 8.0% to 15.2% of genes were assigned into one of the three inheritance

419 categories across the four comparisons (adjusted $p < 0.01$, and see Methods; S7 Table). Further, when
420 inheritance modes could be assigned, we also recorded when the expression level for parent 1 (P1, here
421 ROS-ITi, JP-RRi, MAR-ABi, or MR-VPi) was greater than for parent 2 (P2, always SOL-BEi), as well as
422 when P1 was less than P2.

423 For the comparisons with SOL-BEi, where there were significant expression differences between
424 parental strains (either P1>P2 or P1<P2), dominant inheritance was most common, accounting for 68.4%,
425 72.6% and 76.8% of assignments for MR-VPi, MAR-ABi, and JP-RRi, respectively; in contrast, a lower
426 percentage of genes with dominance was observed in the ROS-ITi comparison (54.6%), for which 43.8%
427 of genes were in the additive category (as compared to 21.6-27.7% for the other three comparisons; Fig 6A
428 and S7 Table). Genes in the transgressive category accounted for a minor proportion of assignments (1.6-
429 3.8%). Additionally, for dominant inheritance there was a bias in the direction of P1 for crosses between
430 JP-RRi, MAR-ABi, and MR-VPi to SOL-BEi (P2) (2.7- to 5.0-fold more than for dominance in the
431 direction of P2), although this trend was not as striking for the ROS-ITi × SOL-BEi comparison (1.3-fold).

432 We also extended this analysis to specifically examine the D+H+P gene set. Although the resulting
433 number of genes for which inheritance could be assigned was relatively small, broadly similar patterns were
434 observed. Intriguingly, however, a trend for dominance in the direction of the parent with lower expression
435 was observed across each of the four comparisons (1.5- to 4.6-fold more genes than for ones with
436 dominance in the direction of the parental line with the higher parental expression level, Fig 6B). We also
437 assessed, for the set of all genes in the additive and dominant categories, the relationship between absolute
438 $\log_2$FC values for genes with significant differences in expression between parents and the relative
439 proportions of additive and dominant inheritance modes. With increasing parental expression differences,
440 the proportion of genes with additive inheritance increased, while the proportion of dominance decreased
441 (Fig 6C). This pattern mirrored what we observed for modes of genetic control, for which *cis* regulation
442 was proportionally greater for genes in bins of increasing magnitude of parental expression differences
443 (categories *cis* and synergism, see Fig 4A). Further, we found that the set of loci featuring *cis* genetic control
444 were enriched for additive inheritance, while *trans* was enriched for dominant inheritance (Fig 6D). A less

445 significant enrichment between *trans* and transgressive inheritance was also observed; in addition, genes
446 controlled by synergism were enriched for additivity, whereas the antagonism category was enriched for
447 transgressive inheritance.

448 We also examined inheritance patterns for specific detoxification genes with documented or
449 suspected roles in acaricide detoxification in *T. urticae*. Because the inheritance classification we adapted
450 from Bao et al. [20] only assigned complete dominance or additivity, many instances of putative partial
451 dominance were not assigned, including for D+H+P genes. To describe inheritance patterns more fully for
452 these and other genes, we assigned partial dominance and its direction using a post hoc approach (see
453 Methods and S7 Table). Among CYP genes with strong *trans*-driven upregulation in one or more
454 comparisons (Fig 5), *CYP392A11* and *CYP392A12* (synergism with *trans* most prominent in JP-RRi and
455 MR-VPi, and for the latter also in MAR-ABi) showed partial dominance in the direction of the parental
456 line with lower expression (SOL-BEi), as did *CYP392A16* (*trans*) in the comparison involving JP-RRi. In
457 contrast, *CYP392A16* (synergism with a large *trans* effect) in the comparisons with MAR-ABi and MR-
458 VPi exhibited additive inheritance. Incomplete dominance in the direction of P2 (SOL-BEi) was also
459 observed for *CYP385A1* in MAR-ABi (*trans*) and for *CYP385B1* (*trans*) in MR-VPi in comparisons to
460 SOL-BEi. For CYP genes with strong *trans*-driven downregulation in comparison to SOL-BEi, additivity
461 was observed for *CYP389C11* (synergism) in JP-RRi, and complete dominance in the direction of P1 was
462 observed in MAR-ABi and MR-VPi (*trans*). Many D+H+P genes exhibited complex patterns depending
463 on the comparison. For instance, while *CYP392D3* was expressed more highly in JP-RRi and MR-VPi (P1)
464 as compared to SOL-BEi (P2), additivity was observed for the former, while partial dominance in the
465 direction of P1 was observed for the latter, and for the MAR-ABi to SOL-BEi comparison over-expression
466 relative to both parents was observed in the F1 (a transgressive up classification) (S7 Table).
467

468 # Discussion

469 With a parental/F1 experimental design we unraveled the genetic control and inheritance of gene expression
470 variation in strains of *T. urticae*, a highly polyphagous mite pest known for its exceptionally rapid evolution
471 of acaricide resistance [25] and host plant adaptation [30–34]. Key findings were that: (1) *trans*-regulatory
472 variation was common; (2) when expression differences of large magnitude were explained by *trans* effects,
473 detoxification genes, including CYPs and DOGs, were enriched; (3) dominance in gene expression
474 inheritance was often observed, and was enriched among genes with *trans*-regulatory control; and (4)
475 dominance or partial dominance was common for many detoxification genes with dramatic expression
476 differences among strains. It should be noted that while each of the five inbred strains included in our study
477 harbored at least one target-site resistance mutation (a toxicodynamic mechanism), some strains like MAR-
478 ABi had multiple target-site resistance mutations, and also higher resistance to many compounds. However,
479 the relationship between target site mutation numbers and acaricide resistance breadth and levels was
480 incomplete, suggesting an important contribution of acaricide detoxification (metabolic resistance, a
481 toxicokinetic mechanism). Indeed, some target-site mutations in *T. urticae* displayed only moderate
482 phenotypic strength after marker-assisted backcrossing onto a different genetic background [55,63],
483 revealing a requirement for detoxification to attain the very high resistance levels encountered in the field.
484 Further, the strains we used captured variation in host plant use representative of that observed in earlier
485 studies with this species [51,54,75].
486

487 ## *Trans* regulation is common in *T. urticae*

488 In all pairwise comparisons, we found that *trans* effects on expression variation were more common than
489 *cis*, even though the latter became more frequent when expression differences between parents were large,
490 as reported in some earlier studies [21,76]. Support for our finding of a higher prevalence of *trans* effects
491 comes as well from inferred modes of inheritance – that is, *trans* effects have been strongly associated with
492 dominance in gene expression ([21], and references therein), and in our study the higher frequency of genes

493 with dominant versus additive inheritance closely mirrored the higher frequency of *trans* versus *cis* effects
494 (this was true among comparisons as well; for instance, for the ROS-ITi x SOL-BEi contrast, relatively
495 fewer *trans* effects and dominance were detected as compared to the other three, compare Fig 3A-D and
496 Fig 4A to Fig 6A). The proportion of *trans* versus *cis* effects has been a focus of many studies, although
497 caution is needed in comparing across studies owing to differences in experimental designs and statistical
498 methods. For instance, our study used more biological replicates than most (five for most comparisons),
499 and more replicates facilitate the detection of differential expression of genes with small fold changes (the
500 group of genes that we found to be most enriched for *trans* effects).

501 Notwithstanding these considerations, our findings are consistent with previous studies in yeast,
502 plants and animals that have used parental/F1 designs with ASE detection to show that while *cis* effects
503 often predominate in interspecific comparisons, over the shorter evolutionary time frame of intraspecific
504 comparisons, *trans* effects are typically, albeit not always, more common ([22], and references therein).
505 Previously, variation in the performance of *T. urticae* strains on different host plants raised the possibility
506 of host race formation within this species. Despite a striking recent example [54,77], comparatively little
507 evidence exists for wide-spread host-race formation in *T. urticae*, where host plant adaptation can occur in
508 as few as five generations [33], and seasonal or yearly movement of *T. urticae* populations among host
509 plants is likely common. Our finding that *trans* regulation is most often observed in *T. urticae* may reflect
510 this, and contrasts to findings in species like the monkeyflower *Erythranthe guttata* (formerly *Mimulus*
511 *guttatus*) and the threespine stickleback fish (*Gasterosteus aculeatus*) for which a predominance of
512 intraspecific *cis* variation has been associated with evolutionary divergent subpopulations (i.e., costal versus
513 inland populations of monkeyflower, and marine versus freshwater populations in the stickleback) [19,78].
514

515 Enrichment for *trans* regulation among detoxification genes

516 Prior studies have revealed large differences in the expression of detoxification genes between *T. urticae*
517 acaricide-susceptible strains and resistant strains that arise rapidly in response to acaricide application [25],

518 or following adaptation to new host plants [30–34]. Selection on *trans*-acting factors is a potential
519 mechanism underlying rapid intraspecific evolution, as many downstream genes impacting the same
520 biological process can be coordinately changed in expression [79,80]. Our study design allowed us to assess
521 this possibility with *T. urticae* strains, including MAR-ABi and MR-VPi, which were derived from outbred
522 progenitor strains that have experienced recent, strong and recurring acaricide selection [33,52,53,69].
523 Strikingly, while genes in detoxification families were not enriched at the extremes of fold changes driven
524 in *cis*, members of the *CYP* and *DOG* families were enriched at the extremes of *trans*-driven expression
525 variation. At the family level, this was especially striking for *DOG*s, for which the near family-wide
526 upregulation in MAR-ABi compared to SOL-BEi was under *trans*-control with only minor contributions
527 from *cis* effects. Recently, several *T. urticae* DOGs including *DOG11* were shown to have broad substrate
528 specificity against aromatic compounds, including plant-derived specialized compounds with roles in plant
529 defense against herbivores [41]. *DOG11* was the most highly over-expressed *DOG* gene in both MAR-ABi
530 and MR-VPi, both of which had comparatively high performance on tomato. RNAi knockdown of *DOG11*
531 in the MR-VPi progenitor strain was recently found to reduce performance on tomato [41], and whether
532 *trans*-mediated upregulation of *DOG11* contributes to the relatively high fitness of these strains on tomato
533 warrants further study. Apart from CYPs and DOGs, it was also striking that specific genes in most other
534 detoxification families, and some associated with host plant use (host use or peptidase gene sets), were also
535 among those with the highest differential expression arising from *trans* control. The relatively low
536 frequency of *trans* effects in ROS-ITi, a strain that like SOL-BEi does not exhibit a high level of acaricide
537 resistance, as compared to the other strains – particularly the multi-resistant MR-VPi and MAR-ABi strains
538 – is consistent with selection on *trans*-regulatory variation in response to acaricide selection (although a
539 less clear relationship was observed for JP-RRi). Our findings are therefore generally consistent with a
540 growing number of studies that suggest that variation in *trans* regulation is important for recently evolved
541 pesticide resistance phenotypes, and potentially for host plant adaptation also. For instance, in the mosquito
542 *Aedes aegypti*, three CYPs were overexpressed in the original strain and in a derived introgressed
543 pyrethroid-resistant strain, and were unlinked from the putative, introgressed resistance locus [81].

544 Notwithstanding findings for the *DOG* family, a robust trend observed across detoxification gene
545 families was that only subsets of genes in families were controlled in *trans*, or that the direction of the
546 expression changes (up or down relative to SOL-BEi) within families or among strains often varied. This
547 finding suggests modular regulation of xenobiotic and host plant associated genes in *T. urticae*. Such
548 modular control might facilitate adaptation to specific host plants and acaricides without wholescale
549 activation of xenobiotic pathways, an outcome that likely entails a fitness cost. In fact, in *T. urticae* evidence
550 for costs to heightened metabolic resistance comes from studies involving *cytochrome P450 reductase*
551 (*CPR*), which encodes the electron donor required for CYP activity. In multiple experimental evolution
552 designs using *T. urticae*, the allele frequencies of *CPR* coding sequence and copy number variants
553 hypothesized to modulate or elevate CPR activity, and that coincided with narrowly-defined intervals for
554 acaricide resistance QTLs, decreased rapidly in the absence of continuous acaricide selection [51–53].
555 While the parental/F1 experimental approach we used to infer genetic control is a powerful design
556 for detecting *trans*-regulatory variation, it cannot identify the loci that are causal. In fact, both the nature of
557 *trans*-acting factors and the genetic variants that underlie them remain enigmatic. For instance, a recent
558 study of variants affecting *trans* regulation of a reporter gene in yeast, while confirming the role of
559 transcription factors, also noted that 90% were in genes outside the known regulatory network of the target
560 gene [82]. Given the paucity of information about the regulation of *T. urticae* detoxification pathways, care
561 should be taken in using candidate gene approaches. However, HR96 genes, of which canonical members
562 encode nuclear hormone receptors with ligand-binding domains (LBDs) and DNA-binding domains
563 (DBDs), have been associated with xenobiotic metabolism in insects such as *Drosophila* [83], and are
564 orthologs of the vertebrate xenosensors PXR and CAR [84]. An HR96 transcription factor (*tetur36g00260*)
565 previously associated with the resistant phenotypes of the MAR-ABi and MR-VPi progenitor strains, and
566 to adaptation to tomato for five generations [33], had *trans*-driven upregulation in all four strains in our
567 study (although antagonistic *cis* effects were also observed in MAR-ABi and JP-RRi). Strikingly, while *D.*
568 *melanogaster* has one HR96 copy, *T. urticae* has eight HR96 homologs (with LBDs and DBDs), and a
569 remarkable 47 genes that have an HR96-like LDB but that lack a DBD [52]. One of the latter

570 (*tetur06g04270*) was at the peak for a resistance QTL for tebufenpyrad resistance in a cross of a strain
571 derived from the MR-VPi progenitor and a susceptible strain [52]. These gene expression and genetic
572 findings, coupled with the exceptional expansion of HR96-like genes in *T. urticae*, raise the possibility that
573 genetic differences at HR96 loci may contribute to the variation in the expression of subsets of
574 detoxification genes observed in our study, although additional work is needed to assess this conjecture.
575

576 **Multiple modes of genetic control for CYPs known to metabolize acaricides**

577 We observed large expression differences of multiple CYPs known to metabolize acaricides included in
578 our study. This was especially true for the CYP392A clade that includes *CYP392A11*, *CYP392A12*, and
579 *CYP392A16* (CYP2 clan). Especially in multi-acaricide resistant MAR-ABi and MR-VPi, these genes were
580 outliers among all CYPs in their very high expression as compared to SOL-BEi, and were in fact among
581 the most strongly differentially expressed of any genes for which we could assign modes of genetic control.
582 As established in earlier work, CYP392A-clade genes have or are likely to have broad substrate specificity.
583 For example, functional expression studies have shown that CYP392A11 can metabolize fenpyroxymate
584 and cyenopyrafen [85], and CYP392A16 has been documented to metabolize abamectin [68] as well as
585 pyflubumide [53]. Additionally, RNAi knockdown of CYP392A16 was found to reduce abamectin
586 resistance in the progenitor of the MAR-ABi strain used in our study [69]. For the CYP392A-clade genes
587 in resistant strains as compared to SOL-BEi, upregulation resulted mainly from *trans* effects. Whether the
588 coordinated upregulation of *CYP392A11*, *CYP392A12*, and *CYP392A16* in resistant strains originates from
589 variation in a shared upstream regulator, and whether such a regulator might also control genes in other
590 families, like *DOG* genes for which variation was controlled predominately in *trans* as well, is an
591 outstanding question.

592 Finally, although *trans* effects were typically largest in magnitude among CYPs, *cis* variation was
593 also observed, including for CYP392A-clade genes in specific pairwise comparisons. In fact, in a prior
594 study promoter variation among two strains, including the MAR-ABi progenitor strain MAR-AB, was

595 demonstrated for *CYP392A16*, with higher expression observed from the MAR-AB promoter than from the
596 promoter of an acaricide-susceptible strain [69]. Adaptive roles for *cis* variants in the control of known
597 detoxification genes in insects have been established or suggested by a number of studies [53,86,87]. For
598 instance, a classic example is the insertion of an Accord transposon into the 5' end of the *Cyp6g1* that
599 confers resistance to DDT in *Drosophila* by elevating *Cyp6g1* expression, and that has spread globally [88].
600 It was striking that synergism was typically observed where both *trans* and *cis* control of CYP392A-clade
601 genes was inferred. However, a moderately large contribution of a *cis* effect was only seen for *CYP392A11*
602 in strain MR-VPi, where it contributed to the remarkably high expression of *CYP392A11* in this strain as
603 compared to SOL-BEi. The extent to which synergism underpins extremes of expression differences in
604 detoxification gene expression is incompletely understood. Nevertheless, our findings suggest that the
605 evolution of high-level, multi-acaricide resistance phenotypes in response to large and repeated acaricide
606 doses may involve selection on multiple variants acting in a reinforcing manner in both *cis* and *trans*. In
607 particular, synergism leading to exceptionally high expression of detoxification genes such as *CYP392A11*
608 that have broad substrate specificities may have outsized importance. Albeit in a different system, Ji et al.
609 [21] reached a similar conclusion based on their finding that reinforcing *cis* and *trans* effects explained the
610 very high expression of several key and potentially rate-limiting genes in defense pathways in maize lines
611 subjected to intense selection for herbivore resistance.
612

613 Dominance or partial dominance is a common inheritance pattern among 614 detoxification genes

615 The ability of advantageous alleles to respond to selection depends on multiple factors, including the degree
616 of dominance. In diploid individuals, dominant mutations are unmasked to selection in the heterozygous
617 state, and hence selection on dominant variants can occur rapidly even when allele frequencies are low (in
618 populations, low frequency alleles are found predominantly in the heterozygous state). Given the rapid
619 evolution of acaricide resistance in *T. urticae*, an expectation might be that the high expression of genes

620 including those in the CYP392A-clade would result from dominance in the direction of resistant strains like
621 MAR-ABi and MR-VPi. While a trend toward dominance of overall gene expression in the direction of
622 these strains was observed, the direction of dominance for D+H+P genes was instead biased toward the
623 parent with lower expression, even if substantial heterogeneity was observed for specific genes. The
624 significance of this trend, as well as if this could be an effect of the single common parent (SOL-BEi) used
625 in crosses, is currently not clear. More speculatively, it might reflect the action of purifying selection in *T.*
626 *urticae* populations on variants that in the heterozygous state result in strong upregulation of detoxification
627 and host-associated genes, but that may also have negative pleiotropic effects (i.e., fitness costs of elevated
628 detoxification in the absence of continuous selection by acaricides or challenging host plants). Regardless,
629 for many detoxification and host plant genes, including *CYP392A11*, *CYP392A12*, and *CYP392A16* as well
630 as many *DOG*s that also had very high *trans*-driven expression in the multi-acaricide resistant strains,
631 partial dominance or additivity was observed. The finding of dominance, or the otherwise intermediate
632 expression of many detoxification genes in F1s as compared to parents (i.e., partial dominance or
633 additivity), suggests that genetic variants underlying expression of xenobiotic resistance or host plant use
634 associated genes should be visible to selection in female *T. urticae* mites (the diploid sex used in our study).
635 This is consistent with the findings of a number of studies that have revealed that phenotypic resistance
636 against pesticides often exhibits incomplete dominance contributed by multiple loci [89–92]. For spider
637 mites, however, an additional factor that likely impacts rapid adaptation is that males are haploid, and in
638 haploid individuals dominance relationships are not relevant. Extrapolation of our findings about gene
639 expression in *T. urticae* females to males will nonetheless require further study.
640

641 **Conclusion**

642 Among *T. urticae* strains, we found that large changes in the expression of genes known or suspected to be
643 important for detoxification or host plant use were underpinned by variation in *trans*-regulatory
644 environments. This was especially striking for genes encoding detoxification enzymes with known and

645 broad substrate specificities, including for CYPs known to detoxify multiple acaricides, as well as for DOGs
646 that have recently been shown to metabolize a broad range of plant-derived aromatic compounds. Our
647 findings position *T. urticae* as an attractive system for future studies to characterize the molecular basis of
648 the control of gene expression variation in xenobiotic and host plant use pathways.
649

650 # Methods

651 ## Mite strains

652 Inbred strains used for genetic and gene expression analyses originated from five *T. urticae* strains: ROS-
653 IT, MAR-AB, MR-VP, JP-RR, and SOL-BE. Briefly, SOL-BE was collected on potato in Belgium in 2018,
654 and ROS-IT was collected from roses in Italy in 2017. The MAR-AB strain originated from a heavily
655 sprayed greenhouse near Athens (Greece) in 2009, and is resistant to abamectin, bifenthrin, clofentezine,
656 hexythiazox, fenbutatin oxide and pyridaben [33]. The MR-VP strain originates from a lab stock originally
657 collected in September 2005 from bean plants in a greenhouse in Brussels, Belgium, and was selected for
658 its extraordinary levels of resistance to mitochondrial electron transport inhibitors of complex I (METI-Is)
659 [48]. The laboratory strain JP-RR was selected for its resistance to electron transport complex II (METI-II)
660 inhibitors (cyanopyrafen, cyflumetofen and pyflubumide) from its parental strain JP-R, as described by
661 Khalighi et al. [49]. To avoid the confounding effect of heterozygosity on downstream studies of the control
662 of gene regulation, the strains were inbred via mother-son mating (performed as described by Bryon et al.
663 [47]) for 7 to 9 generations to produce the respective inbred strains (postfixed with the "i" for inbred
664 designation; ROS-ITi, MAR-ABi, MR-VPi, JP-RRi, and SOL-BEi). The resulting inbred strains were
665 expanded from a single female until the population permitted experimental use. All strains were maintained
666 on potted kidney bean plants (*Phaseolus vulgaris* var. 'Prelude') at 25°C (±0.5°C), 60% relative humidity,
667 and 16:8 h light:dark photoperiod.
668

669 ## Bioassays

670 Acaricide resistance levels of all inbred strains were determined in bioassays as previously described by
671 Van Pottelberge et al. [48]. Serial dilutions of acaricides and water (negative control) were tested in four
672 replicates of 20-30 adult female mites on 9 cm^2 square leaf disks on wet cotton. Using a Cornelis spray
673 tower, 800 µl of fluid was sprayed on each leaf-disk at a pressure of 1 bar (1.5 mg fluid deposition per cm^2).
674 The acaricides used and the corresponding IRAC Mode of Action (MoA) and time of mortality assessment
675 are listed in S1 Table. Dose-response curves, LC_{50}-values, and their 95% confidence intervals were
676 calculated using POLO-plus software (version 2.0) [93]; after earlier work, significant differences were
677 assessed when 95% confidence intervals did not overlap [94].
678

679 ## Host performance assays

680 The fitness of inbred strains ROS-ITi, JP-RRi, MAR-ABi, and MR-VPi was assessed on five different
681 hosts: bean (*Phaseolus vulgaris* var. 'Prelude'), tomato (*Solanum lycopersum* var. 'Moneymaker'), potato
682 (*Solanum tuberosum* var. 'Bintje'), cucumber (*Cucumis sativus* var. 'Ventura') and prune (*Prunus*
683 *domestica* var. 'Brompton'). This was evaluated by placing leaf discs of the respective host plant (4 cm^2)
684 on wet cotton wool with the adaxial side up. Discs were infested with ten female adults (4-5 days old) per
685 disc with at least four replicates per strain and per host. After three days, the total number of eggs on each
686 leaf disc was recorded. Statistical differences among strains by host plant were assessed by analysis of
687 variance (ANOVA); where significant differences were observed, post-hoc Tukey tests were applied.
688 Analyses were performed in R (version 4.0.4) [95].
689

690 ## DNA extractions and sequencing

691 For each of the parental inbred strains, DNA was isolated from a pool of 400 adult female mites by phenol-
692 chloroform extraction as described in Villacis-Perez et al. [54]. DNA concentration and purity were
693 measured using a spectrophotometer (DeNovix, USA). Integrity of the DNA samples was checked via gel

694 electrophoresis (2% agarose gel; 30 min; 100V). From the resulting DNA samples of the MAR-ABi, MR-
695 VPi, JP-RRi, and SOL-BEi strains, Illumina DNA-seq libraries were constructed using the Illumina TruSeq
696 Nano DNA library prep kit, and subsequently sequenced with the Illumina HiSeq2500 technology (paired-
697 end reads of 125 bp) at the Huntsman Cancer Institute of the University of Utah (Salt Lake City, Utah,
698 USA). From the DNA extracted for ROS-ITi, an Illumina library was constructed using the Illumina
699 NEBNext Ultra II DNA library prep kit and sequenced with the Illumina HiSeq3000 technology (paired-
700 end reads of 150 bp) at NXTGNT (Ghent, Belgium).
701

702 DNA read alignments and PCA

703 Genomic reads from each of the five inbred strains were aligned to the *T. urticae* London reference genome
704 [51] using BWA (version 0.7.17-r1188) [96]. Sorting and indexing of the resulting BAM files were
705 performed with SAMtools (version 1.9) [97], and duplicate reads were marked with Picard (version
706 2.18.11-SNAPSHOT) (http://broadinstitute.github.io/picard/). Genetic variants across all strains were
707 predicted with the Genomic Analysis Toolkit (GATK) following the best practices workflow (version
708 4.0.7.0) [98,99]. To assess potential acaricide resistance target-site changes, potential effects of predicted
709 variants on amino acid sequences were assessed using a custom-built database with SNPeff (version 4.3L)
710 [100]. The database was constructed based on the coding exons (CDS) from the June 2016 ORCAE GFF
711 annotation [101]. To describe relatedness among strains, a principal component analysis (PCA) was
712 performed after filtering the resultant variant call format (VCF) file with additional criteria to further
713 eliminate aberrant predictions. The filtering criteria were adapted from previous studies [51]. Briefly, each
714 SNP included in the PCA had to have the quality score normalized by allele depth (QD in the VCF file) of
715 at least 2, mean mapping quality score (MQ) of at least 50, and strand odds ratio (SOR) below 3. Mapping
716 quality rank sum (MQRankSum) and rank sum for relative positioning of alleles in reads
717 (ReadPosRankSumTest) both had to be at least −8 when present. Finally, coverage (as indicated by the total
718 depth per allele per sample [AD] field in the VCF file) had to be within 25% and 150% of the sample's

719 genome-wide mean SNP read coverage (to restrict the analysis to variants in putative single copy regions).
720 The PCA was carried out in R (version 3.5.2) [95] using SNPRelate (version 0.16.1) [102] with the
721 "autosome.only=FALSE" option. The PCA was performed on the GDS file converted from the VCF using
722 gdsfmt (version 0.18.1) [102,103] with the option "method=copy.num.of.ref" (which includes all SNPs).
723 Further, we confirmed that the five strains were in fact isogenic, as expected for inbred strains, by
724 determining the fraction of variable SNPs in each parental strain that were fixed (i.e., homozygous; see
725 Results); to do this, we used the approach of Villacis-Perez et al. [54].
726

727 ## Genetic crosses for genetic mode of expression control determination

728 To investigate expression variation between strains and its genetic mode of control and inheritance, we
729 adapted a parental/F1 design that has been used previously [9,14,15,20,104]. To do this, we crossed 40
730 virgin females of strains ROS-ITi, JP-RRi, MAR-ABi, and MR-VPi to 40 males of strain SOL-BEi to
731 generate four sets of F1s; in parallel, we produced matching progeny for each parental strain. The crosses
732 to generate F1 and parental strain females were performed with 5-fold biological replication, except for
733 MAR-ABi, JP-RRi, and the JP-RRi × SOL-BEi F1s, for which four biological replicates were obtained.
734 For each replicate (F1 or parental), 100-120 adult female mites at four days of age were collected, except
735 for the JP-RRi × SOL-BEi F1s for which females of 4-7 days old were collected. Immediately after mite
736 collection, samples were frozen in dry ice until storage at -80°C.
737

738 ## RNA extractions and sequencing

739 For each sample of 100-120 adult female mites (a parental or F1 replicate), total RNA was extracted from
740 the frozen mite samples (-80°C) using the RNeasy Plus Mini Kit (Qiagen, Belgium) according to the
741 manufacturer's Quick-Start Protocol. Samples were kept on dry ice until adding the first buffer of the
742 RNeasy Plus Mini Kit. RNA concentration and purity were measured using a DeNovix spectrophotometer
743 (DeNovix, USA). The integrity of the RNA-sample was checked via gel electrophoresis (1% agarose gel;

744 30 min; 100 V). Illumina libraries were constructed using the Illumina TruSeq stranded mRNA library prep
745 kit and sequenced on the Illumina HiSeq3000 platform (paired-end reads of 150 bp). Library construction
746 and sequencing was conducted at NXTGNT (Ghent, Belgium).
747

748 RNA-seq read alignments and PCA

749 RNA-seq reads from parents and F1 samples were aligned to the London reference genome using GSNAP
750 (version 2018-07-04) [73,74], an aligner that incorporates SNP information to reduce reference bias in the
751 alignment of reads derived from non-reference samples. The alignments were performed with known splice
752 sites supplied to GSNAP using the GFF annotation of Wybouw et al. [51] with novel splice discovery
753 enabled and with the options "--localsplicedist=50000 --novelend-splicedist=50000 --pairmax-rna=50000
754 --gmap-mode=all". Variant information was supplied to GSNAP in a sample-dependent manner. Briefly,
755 pairwise VCF files were generated and supplied to GSNAP for the respective alignments. For instance, for
756 alignments of reads from F1s from the ROS-ITi × SOL-BEi cross, a VCF file was supplied to GSNAP that
757 contained only the SNP variants identified for the ROS-ITi and SOL-BEi strains as compared to the London
758 reference genome (see section "DNA read alignments and PCA"). Read counts per gene per genotype and
759 biological replicate were then assessed with HTSeq version 0.11.2 [105]. To assess global patterns of gene
760 expression, as well as variation among replicates for all parental strain and F1 samples, a PCA was
761 performed on the resulting expression data using DESeq2 (version 1.22.2) [106].
762

763 Selection of putatively intact and single copy gene sets

764 For pairwise strain expression comparisons to detect ASE (i.e., for each set of two parent strains and the
765 respective F1), we first identified genes that were putatively intact and single copy in each pair of parents.
766 To select the "intact+single copy" gene sets, we used both genomic read and RNA-seq read data. With
767 aligned genomic reads on a per strain basis, we detected putative copy number variation using read
768 coverage. To do this, median per-base DNA read coverage was determined across the three *T. urticae*

769 chromosomes. Briefly, pysam's "count coverage" function was used with default settings (pysam version
770 0.15; https://pysam.readthedocs.io/en/latest/api.html), and the median of all non-zero values was recovered.
771 In addition, the coverage for each CDS exon of a gene was assessed using the same approach with reads
772 that mapped in a proper pair and with a MQ score of 40 (the maximum quality score). Genes that had a
773 coverage below 5% or above 150% of the genome-wide median within any CDS exon were considered to
774 be copy variable in the respective strain. In addition, GATK variant predictions (single nucleotide and small
775 indel differences) were assessed for impacts on genes by substituting them into the London reference
776 sequence on a per strain basis. The respective CDS sequences for each gene were then extracted and joined
777 to determine the largest open reading frame (ORF) accounting for the strand on which the gene was
778 annotated ("+" or "-" in the GFF annotation file). Biopython version 1.74 was then used for translations
779 [107]. To account for variation at gene ends that may be neutral, such as nearby alternative start or stop
780 codons, sequences 12 bp upstream of the first CDS exon and 12 bp downstream of the last CDS exon were
781 included in the ORF prediction.

782 In order for a gene to be considered for inclusion in downstream ASE analyses involving a pair of
783 strains, based on genomic read data the following criteria had to be met: (1) the gene had to be putatively
784 single copy in both strains as assessed from DNA read coverage, (2) the longest ORF of the gene had to
785 contain a putative start and stop codon in both strains, and (3) there had to be an amino acid sequence match
786 of at least 90% for the predicted protein sequences between the two strains. For assessing the latter, global
787 alignments were performed using the pairwise2 module in Biopython; identical amino acids were given an
788 assigned a score of 1, and the sum of scores was divided by the alignment length (the longer of the two
789 sequences used in each pairwise comparison) to determine percent identity.

790 Additionally, to be considered in an ASE analysis between a pair of parents, a gene had to pass a
791 final filter based on RNA-seq read alignment data. Briefly, apparent heterozygosity in aligned RNA-seq
792 reads, if observed in inbred strains, may result from cross-mapping of similar, duplicate sequences to a
793 single sequence in the reference genome used for alignment. To detect this, for each inbred strain we
794 combined RNA-seq reads from all replicates (i.e., from all BAM files for a given parental genotype) and

795 selected reads in proper pairs with MQ values of 40. For each position within a CDS, we required that the
796 minor allele frequency could be at most 0.1 (in assessing base calls in reads by position, a minimum base
797 quality score threshold of 30 was used). If a gene failed this criterium in either of the two parents, it was
798 not included in the respective intact+single copy gene set.
799

800 **Assignment of parent of origin to aligned RNA-seq reads**

801 ASE analyses based on RNA-seq alignments require that individual reads are assigned to a parent of origin
802 based on variants in transcribed regions (reads that align to identical sequences between the two parent
803 strains are uninformative). For F1 samples, we developed an in-house Python program (available at
804 https://github.com/akurlovs/ase) that employed pysam (version 0.15) to distinguish reads derived from one
805 or the other parent for a respective F1 sample. Briefly, SNPs that distinguished the two parents of a given
806 F1 were first recovered from the respective pairwise VCF files (see section "RNA-seq read alignments and
807 PCA"; an MQ value of 40 or more was applied for SNP selection). F1 RNA-seq reads that were mapped in
808 a proper pair with read-level MQ values of 40 (the maximum values assigned with GSNAP) were then
809 recovered and written to parent of origin BAM files if reads contained bases at SNP sites specific to one of
810 the two parents of the F1 (reads for which the parent of origin could not be assigned were discarded). The
811 same workflow was also applied to RNA-seq samples of the respective parents to generate matching read
812 alignment data (that is, only parental reads that overlapped the same informative SNP sites used in the F1
813 analyses were included). Following parent of origin read assignment, reads within CDS exons were counted
814 from the resulting BAM files with HTSeq.
815

816 **Assignment of mode of genetic control for gene expression variation**

817 By assessing differential expression between parent of origin expression in F1s (ASE, *cis* effects only) and
818 differential expression between the parents (which can arise from both *cis* and *trans* effects), we classified
819 genes into seven control modes adapted from McManus et al. [14]: "*cis*", "*trans*", "synergism" (*cis* and

820 *trans* effects acting in the same direction), "antagonism" (*cis* and *trans* effects acting in opposite directions),
821 "compensatory" (a special case of antagonism for which significant *cis* and *trans* effects offset such that
822 there is no differential expression between parents), "conserved" (no parental expression differences and
823 no significant *cis* or *trans* effects), and "ambiguous" (genes that do not fall in any of the above categories).
824 Differential expression analyses between parents of an F1 and between parent-of-origin reads for the
825 respective F1s were both performed with DESeq2 with the alpha value set to the default of 0.1 (i.e., an
826 adjusted *p*-value threshold of 0.1 was used). Genes with average base mean expression values of below 20,
827 as determined in the respective DESeq2 analyses, were excluded from subsequent analyses for assignment
828 of genetic mode of control. We then assigned significant *trans* effects by applying Fisher's exact test to
829 DESeq2 normalized allele-specific count ratios of F1 versus normalized count ratios of respective parental
830 strains for genes in "intact+single copy" gene sets by pairwise comparison; for a given cross, *p*-values for
831 *trans* assignment were then Benjamini-Hochberg adjusted for multiple comparisons and those for which
832 the adjusted-*p* was less than 0.1 were considered significant. For performing tests for significant *trans*
833 effects, the DESeq2 normalized expression data across replicates was summed, and resulting values were
834 weighted by the number of replicates if different numbers of replicates were available for given pairwise
835 comparisons. Fold changes between parents, as well as for F1s (*cis* effects), were from estimates from the
836 DESeq2 analyses ($\log_2$FC values); the contribution of *trans* effects to fold changes was estimated by
837 subtracting the respective $\log_2$FC values for the F1 parent-specific allele counts (ASE analyses) from the
838 $\log_2$FC values for the two parental strains. Further, prior to calculating $\log_2$FC values associated with *trans*
839 regulation, those for the parental and F1s analyses were shrunk using ashr (version 2.2-32) [108] to prevent
840 lowly expressed genes from confounding the results.
841

842 ## Inheritance of gene expression variation

843 By comparing expression of genes between the parental strains and that of respective hybrid F1 offspring,
844 the inheritance mode for expression of individual genes was inferred. For this purpose, we adapted the

845 methodology from Bao et al. [20]. The inheritance modes were classified into the following categories:
846 "additive" (expression in F1s is equally between that of the two parental strains), "dominant" (F1 expression
847 is equal to that of either the maternal or paternal strain), and "transgressive" (F1 expression falling outside
848 the parental range). Note that while additivity and dominance are observed when there are significant
849 expression differences between parental strains, transgressive inheritance can be observed even if there is
850 no expression divergence between parents. For this inheritance mode classification, we performed four
851 rounds of differential gene expression analyses using DESeq2 (version 1.28). Input for the analyses was
852 total gene read counts for all genes (all replicates were used for every genotype, parental or F1); for the
853 following, P1 represents the varying parents (ROS-ITi, JP-RRi, MAR-ABi, and MR-VPi) and P2 represents
854 the SOL-BEi strain. The first differential expression analysis was performed using the parents, and
855 significantly differentially expressed genes between parents ($P_1 \neq P_2$) were identified with the following
856 criteria: (1) *p*-adjusted < 0.01, (2) absolute $\log_2$FC > 0.5, and (3) baseMean > 15 (to remove lowly expressed
857 genes from the analysis). The second and third rounds of analyses were performed by comparing F1
858 expression to the respective two parental strains using a significance cutoff of *p*-adjusted < 0.01. The fourth
859 analysis was performed by comparing F1 expression to the midpoint of parental strains (*p*-adjusted < 0.01;
860 see Bao et al. [20] for methods). In the case of P1≠P2, if F1=P1 or F1=P2 only, genes were classified into
861 the dominant category in the direction of one or the other parent, and for F1=(P1+P2)/2 only, genes were
862 classified into the additive inheritance category. The criteria for transgressive inheritance was (1) F1>P1
863 and F1>P2, or (2) F1<P1 and F1<P2.

864 The strict criteria we used to assign genes into pure dominant, additive, and transgressive categories
865 overlooked a large number of genes showing partial dominance when $P_1 \neq P_2$. To more fully describe
866 inheritance, we used the formula of Stone [109] to assign partial dominance and its direction:

867 $$\mathrm{H} = \frac{2F1 - P1 - P2}{P1 - P2}$$

868 where F1, P1 and P2 represent respective mean expression values of each genotype (after normalization by
869 DESeq2). When $0 < H < 1$, incomplete dominant in the direction of P1 was assigned; when $-1 < H < 0$,
870 incomplete dominant in the direction of P2 was assigned.

871 Association analysis between inheritance mode (excluding partial dominance categories) and mode
872 of gene regulatory control was based on Pearson's Chi-squared test using the chisq.test function in R v4.0
873 [95] with data across all four comparisons for the subset of genes where both inheritance mode and gene
874 regulatory modes were assigned.

875

876 Detoxification and host plant associated genes

877 "Detoxification genes" were defined as genes belonging to gene families involved in detoxification and/or
878 host plant adaptation, although it should be noted that not every gene in these families plays a role in the
879 detoxification process. For ATP-binding cassette transporters (ABCs), carboxyl/cholinesterases (CCEs),
880 glutathione S-transferases (GSTs), intradiol ring-cleavage dioxygenases (DOGs), and UDP-
881 glycosyltransferases (UGTs) gene family information was obtained directly from the *T. urticae* three-
882 chromosome gene information file [51]. Since the release of the 2016 annotation, Snoeck et al. [46]
883 reannotated short-chain dehydrogenases (SDRs) and PLAT-domain proteins in *T. urtica*e and gene
884 identifiers for those families were obtained from "Tables *S7* and *S8*" in their manuscript (only complete
885 sequences were used). In addition, genes belonging to the cytochrome P450 (CYP) family and the major
886 facilitator superfamily (MFS) were identified using InterProScan (version 5.32-71.0) [110], which was run
887 on the peptides specified in the June 2016 ORCAE annotation [101], by extracting genes annotated as
888 "IPR036396" ("Cytochrome P450 superfamily") and "IPR011701" ("Major facilitator superfamily", Pfam
889 category identified as upregulated upon host acclimation in Snoeck et al. [46]), respectively. The lipocalin
890 gene set came from "Table S2" in Dermauw et al. [33].

891 The 318 "core" genes that were highly and consistently differentially expressed upon host transfer
892 in Wybouw et al. [34] were also included and referred to as "host" genes. The list of peptidases was obtained

893 from Grbić' et al.'s [42] supplementary list "S6.1.9. Cysteine peptidase genes" and "S6.1.10. Aspartic
894 peptidase genes", except for *tetur13g02490* which was replaced by *tetur13g02500* (a name change in later
895 annotations). See S5 Table for resulting family and host classifications for genes.
896

897 Gene ontology (GO) enrichment analysis

898 Gene ontology enrichment analyses (molecular function, MF) for genes showing extreme upregulating or
899 downregulating *cis* and *trans* effects – defined as those in the top 2.5% and bottom 2.5% for *cis* and *trans*
900 evaluated independently – were performed on the GO categories annotated on the June 2016 *T. urticae*
901 ORCAE annotation [101] by InterProScan (version 5.32-71.0) [110]. For the pairwise comparisons to SOL-
902 BEi, top indicates upregulation relative to SOL-BEi, and bottom indicates downregulation relative to SOL-
903 BEi. The distributions for *cis* and *trans* were established based on the maximum contributions of *cis* or
904 *trans* for given genes assessed across all four comparisons; where a gene was controlled by combinations
905 of *cis* and *trans* (e.g., control by synergism), the contributions of each of *cis* and *trans* were considered
906 independently in constructing the respective distributions. For GO categories that included ten or more
907 genes in the sample being tested, we determined whether the tails of the distributions contained a
908 disproportionately high number of genes belonging to the GO category by performing Fisher's exact tests
909 (the comparison was to all genes in the respective distributions). The resulting *p*-values were Benjamini-
910 Hochberg-corrected to adjust for multiple comparisons and enriched GO terms were identified where the
911 adjusted *p*-values were < 0.05.
912

913 Phylogenetic constructions of detoxification gene families

914 Neighbor-joining trees were constructed for the CYP, DOG, lipocalin, and SDR detoxification gene
915 families. Amino acid sequences for the respective families were extracted from the June 2016 annotation
916 [101] and aligned using MUSCLE (version 3.8.1551) [111]. The scikit-bio Python package (version 0.5.4)
917 (https://github.com/biocore/scikit-bio) was used to construct neighbor-joining trees based on a distance

matrix between the amino acid sequences. The trees were visualized alongside heatmaps displaying differential expression magnitude (log_2FC) between parental strains, as well as expression explained by *cis* and *trans* effects, using the Python package ete3 (version 3.1.1) [112] and matplotlib [113]. For display, a gene was included in a given pairwise comparison if a genetic mode of control could be assessed.

Acknowledgements

We thank Ibrahim Ismaeil for help with inbreeding and bioassays, and Robert Greenhalgh for assistance with managing read data. This work was supported by grant 772026-POLYADAPT, 773902–SuperPests (Research Council (ERC) under the European Union's Horizon 2020 research and innovation program) and BOFSTA2017003701 (Bijzonder Onderzoeksfonds UGent) to TVL, and by incentive funds from the University of Utah to RMC.

Data availability statement

DNA and RNA-seq read data have been deposited to NCBI under identifiers PRJNA799176 and PRJNA801103, respectively. Pairwise strain variant call data, and read count data, have been deposited to figshare (https://doi.org/10.6084/m9.figshare.20291175.v1).

Competing interests

The authors declare no competing interests.

References

1. Slatkin M. Linkage disequilibrium — understanding the evolutionary past and mapping the medical future. Nat Rev Genet. 2008;9: 477–485. doi:10.1038/nrg2361

941 2. Charlesworth B. Effective population size and patterns of molecular evolution and
942 variation. Nat Rev Genet. 2009;10: 195–205. doi:10.1038/nrg2526

943 3. Feuk L, Carson AR, Scherer SW. Structural variation in the human genome. Nat Rev
944 Genet. 2006;7: 85–97. doi:10.1038/nrg1767

945 4. Alkan C, Coe BP, Eichler EE. Genome structural variation discovery and genotyping. Nat
946 Rev Genet. 2011;12: 363–376. doi:10.1038/nrg2958

947 5. Frary A, Nesbitt TC, Grandillo S, Knaap E, Cong B, Liu J, et al. *fw2.2*: a quantitative trait
948 locus key to the evolution of tomato fruit size. Science. 2000;289: 85–88.
949 doi:10.1126/science.289.5476.85

950 6. Shapiro MD, Marks ME, Peichel CL, Blackman BK, Nereng KS, Jónsson B, et al. Genetic
951 and developmental basis of evolutionary pelvic reduction in threespine sticklebacks.
952 Nature. 2004;428: 717–723. doi:10.1038/nature02415

953 7. Gompel N, Prud'homme B, Wittkopp PJ, Kassner VA, Carroll SB. Chance caught on the
954 wing: *cis*-regulatory evolution and the origin of pigment patterns in *Drosophila*. Nature.
955 2005;433: 481–487. doi:10.1038/nature03235

956 8. Clark RM, Wagler TN, Quijada P, Doebley J. A distant upstream enhancer at the maize
957 domestication gene *tb1* has pleiotropic effects on plant and inflorescent architecture. Nat
958 Genet. 2006;38: 594–597. doi:10.1038/ng1784

959 9. Wittkopp PJ, Haerum BK, Clark AG. Evolutionary changes in *cis* and *trans* gene
960 regulation. Nature. 2004;430: 85–88. doi:10.1038/nature02698

961 10. Wang Z, Gerstein M, Snyder M. RNA-Seq: a revolutionary tool for transcriptomics. Nat
962 Rev Genet. 2009;10: 57–63. doi:10.1038/nrg2484

963 11. Albert FW, Kruglyak L. The role of regulatory variation in complex traits and disease. Nat
964 Rev Genet. 2015;16: 197–212. doi:10.1038/nrg3891

965 12. Landry CR, Wittkopp PJ, Taubes CH, Ranz JM, Clark AG, Hartl DL. Compensatory *cis*-
966 *trans* evolution and the dysregulation of gene expression in interspecific hybrids of
967 *Drosophila*. Genetics. 2005;171: 1813–1822. doi:10.1534/genetics.105.047449

968 13. Tirosh I, Reikhav S, Levy AA, Barkai N. A yeast hybrid provides insight into the
969 evolution of gene expression regulation. Science. 2009;324: 659–662.
970 doi:10.1126/science.1169766

971 14. McManus CJ, Coolon JD, Duff MO, Eipper-Mains J, Graveley BR, Wittkopp PJ.
972 Regulatory divergence in *Drosophila* revealed by mRNA-seq. Genome Res. 2010;20:
973 816–825. doi:10.1101/gr.102491.109

974 15. Shi X, Ng DW-K, Zhang C, Comai L, Ye W, Jeffrey Chen Z. *Cis*- and *trans*-regulatory
975 divergence between progenitor species determines gene-expression novelty in *Arabidopsis*
976 *allopolyploids*. Nat Commun. 2012;3: 950. doi:10.1038/ncomms1954

977 16. Schaefke B, Emerson JJ, Wang T-Y, Lu M-YJ, Hsieh L-C, Li W-H. Inheritance of gene
978 expression level and selective constraints on *trans*- and *cis*-regulatory changes in yeast.
979 Mol Biol Evol. 2013;30: 2121–2133. doi:10.1093/molbev/mst114

980 17. Waters AJ, Makarevitch I, Noshay J, Burghardt LT, Hirsch CN, Hirsch CD, et al. Natural
981 variation for gene expression responses to abiotic stress in maize. Plant J. 2017;89: 706–
982 717. doi:10.1111/tpj.13414

983 18. Glaser-Schmitt A, Zečić A, Parsch J. Gene regulatory variation in *Drosophila*
984 *melanogaster* renal tissue. Genetics. 2018;210: 287–301. doi:10.1534/genetics.118.301073

985 19. Verta J-P, Jones FC. Predominance of *cis*-regulatory changes in parallel expression
986 divergence of sticklebacks. Elife. 2019;8: e43785. doi:10.7554/eLife.43785

987 20. Bao Y, Hu G, Grover CE, Conover J, Yuan D, Wendel JF. Unraveling *cis* and *trans*
988 regulatory evolution during cotton domestication. Nat Commun. 2019;10: 5399.
989 doi:10.1038/s41467-019-13386-w

990 21. Ji M, Bui H, Ramirez RA, Clark RM. Concerted *cis* and *trans* effects underpin heightened
991 defense gene expression in multi-herbivore-resistant maize lines. Plant J. 2022.
992 doi:10.1111/tpj.15812

993 22. Hill MS, Vande Zande P, Wittkopp PJ. Molecular and evolutionary processes generating
994 variation in gene expression. Nat Rev Genet. 2021;22: 203–215. doi:10.1038/s41576-020-
995 00304-w

996 23. Van Leeuwen T, Vontas J, Tsagkarakou A, Dermauw W, Tirry L. Acaricide resistance
997 mechanisms in the two-spotted spider mite *Tetranychus urticae* and other important Acari:
998 A review. Insect Biochem Mol Biol. 2010;40: 563–572. doi:10.1016/j.ibmb.2010.05.008

999 24. Feyereisen R, Dermauw W, Van Leeuwen T. Genotype to phenotype, the molecular and
1000 physiological dimensions of resistance in arthropods. Pestic Biochem Physiol. 2015;121:
1001 61–77. doi:10.1016/j.pestbp.2015.01.004

1002 25. Van Leeuwen T, Dermauw W. The molecular evolution of xenobiotic metabolism and
1003 resistance in chelicerate mites. Annu Rev Entomol. 2016;61: 475–498.
1004 doi:10.1146/annurev-ento-010715-023907

1005 26. Hawkins NJ, Bass C, Dixon A, Neve P. The evolutionary origins of pesticide resistance.
1006 Biol Rev. 2019;94: 135–155. doi:10.1111/brv.12440

1007 27. Roush RT, McKenzie JA. Ecological genetics of insecticide and acaricide resistance.
1008 Annu Rev Entomol. 1987;32: 361–380. doi:10.1146/annurev.en.32.010187.002045

1009 28. Nkongolo KK, Quick JS, Limin AE, Fowler DB. Sources and inheritance of resistance to
1010 Russian wheat aphid in *Triticum* species amphiploids and *Triticum tauschii*. Can J Plant
1011 Sci. 1991;71: 703–708. doi:10.4141/cjps91-103

1012 29. Paolino A, Gassmann A. Assessment of inheritance and fitness costs associated with field-
1013 evolved resistance to Cry3Bb1 maize by Western corn rootworm. Toxins. 2017;9: 159.
1014 doi:10.3390/toxins9050159

1015 30. Gould F. Rapid host range evolution in a population of the phytophagous mite
1016 *Tetranychus urticae* Koch. Evolution. 1979;33: 791. doi:10.2307/2407646

1017 31. Fry JD. Evolutionary adaptation to host plants in a laboratory population of the
1018 phytophagous mite *Tetranychus urticae* Koch. Oecologia. 1989;81: 559–565.

1019 32. Magalhães S, Fayard J, Janssen A, Carbonell D, Olivieri I. Adaptation in a spider mite
1020 population after long-term evolution on a single host plant: Host plant adaptation in spider
1021 mites. J Evol Biol. 2007;20: 2016–2027. doi:10.1111/j.1420-9101.2007.01365.x

1022 33. Dermauw W, Wybouw N, Rombauts S, Menten B, Vontas J, Grbić M, et al. A link
1023 between host plant adaptation and pesticide resistance in the polyphagous spider mite
1024 *Tetranychus urticae*. Proc Natl Acad Sci USA. 2013;110: E113–E122.
1025 doi:10.1073/pnas.1213214110

1026 34. Wybouw N, Zhurov V, Martel C, Bruinsma KA, Hendrickx F, Grbić V, et al. Adaptation
1027 of a polyphagous herbivore to a novel host plant extensively shapes the transcriptome of
1028 herbivore and host. Mol Ecol. 2015;24: 4647–4663. doi:10.1111/mec.13330

1029 35. Krieger RI, Feeny PP, Wilkinson CF. Detoxication enzymes in the guts of caterpillars: an
1030 evolutionary answer to plant defenses? Science. 1971;172: 579–581.
1031 doi:10.1126/science.172.3983.579

1032 36. Dermauw W, Osborne EJ, Clark RM, Grbić M, Tirry L, Van Leeuwen T. A burst of ABC
1033 genes in the genome of the polyphagous spider mite *Tetranychus urticae*. BMC Genomics.
1034 2013;14: 317. doi:10.1186/1471-2164-14-317

1035 37. Dermauw W, Van Leeuwen T, Feyereisen R. Diversity and evolution of the P450 family
1036 in arthropods. Insect Biochem Mol Biol. 2020;127: 103490.
1037 doi:10.1016/j.ibmb.2020.103490

1038 38. Gloss AD, Vassão DG, Hailey AL, Nelson Dittrich AC, Schramm K, Reichelt M, et al.
1039 Evolution in an ancient detoxification pathway is coupled with a transition to herbivory in
1040 the Drosophilidae. Mol Biol Evol. 2014;31: 2441–2456. doi:10.1093/molbev/msu201

1041 39. Heidel-Fischer HM, Vogel H. Molecular mechanisms of insect adaptation to plant
1042 secondary compounds. Curr Opin Insect Sci. 2015;8: 8–14.
1043 doi:10.1016/j.cois.2015.02.004

1044 40. Pavlidi N, Vontas J, Van Leeuwen T. The role of glutathione S-transferases (GSTs) in
1045 insecticide resistance in crop pests and disease vectors. Curr Opin Insect Sci. 2018;27: 97–
1046 102. doi:10.1016/j.cois.2018.04.007

1047 41. Njiru C, Xue W, De Rouck S, Alba JM, Kant MR, Chruszcz M, et al. Intradiol ring
1048 cleavage dioxygenases from herbivorous spider mites as a new detoxification enzyme
1049 family in animals. BMC Biol. 2022;20: 131. doi:10.1186/s12915-022-01323-1

1050 42. Grbić M, Van Leeuwen T, Clark RM, Rombauts S, Rouzé P, Grbić V, et al. The genome
1051 of *Tetranychus urticae* reveals herbivorous pest adaptations. Nature. 2011;479: 487–492.
1052 doi:10.1038/nature10640

1053 43. Wybouw N, Van Leeuwen T, Dermauw W. A massive incorporation of microbial genes
1054 into the genome of *Tetranychus urticae*, a polyphagous arthropod herbivore. Insect Mol
1055 Biol. 2018;27: 333–351. doi:10.1111/imb.12374

1056 44. Ahn S-J, Dermauw W, Wybouw N, Heckel DG, Van Leeuwen T. Bacterial origin of a
1057 diverse family of UDP-glycosyltransferase genes in the *Tetranychus urticae* genome.
1058 Insect Biochem Mol Biol. 2014;50: 43–57. doi:10.1016/j.ibmb.2014.04.003

1059 45. Wybouw N, Pauchet Y, Heckel DG, Van Leeuwen T. Horizontal gene transfer contributes
1060 to the evolution of arthropod herbivory. Genome Biol Evol. 2016;8: 1785–1801.
1061 doi:10.1093/gbe/evw119

1062 46. Snoeck S, Wybouw N, Van Leeuwen T, Dermauw W. Transcriptomic plasticity in the
1063 arthropod generalist *Tetranychus urticae* upon long-term acclimation to different host
1064 plants. G3. 2018; g3.200585.2018. doi:10.1534/g3.118.200585

1065 47. Bryon A, Kurlovs AH, Dermauw W, Greenhalgh R, Riga M, Grbić M, et al. Disruption of
1066 a horizontally transferred phytoene desaturase abolishes carotenoid accumulation and
1067 diapause in *Tetranychus urticae*. Proc Natl Acad Sci USA. 2017;114: E5871–E5880.
1068 doi:10.1073/pnas.1706865114

1069 48. Van Pottelberge S, Van Leeuwen T, Nauen R, Tirry L. Resistance mechanisms to
1070 mitochondrial electron transport inhibitors in a field-collected strain of *Tetranychus*
1071 *urticae* Koch (Acari: Tetranychidae). Bull Entomol Res. 2009;99: 23.
1072 doi:10.1017/S0007485308006081

1073 49. Khalighi M, Dermauw W, Wybouw N, Bajda S, Osakabe M, Tirry L, et al. Molecular
1074 analysis of cyenopyrafen resistance in the two-spotted spider mite *Tetranychus urticae*.
1075 Pest Manag Sci. 2016;72: 103–112. doi:10.1002/ps.4071

1076 50. Xue W, Snoeck S, Njiru C, Inak E, Dermauw W, Van Leeuwen T. Geographical
1077 distribution and molecular insights into abamectin and milbemectin cross-resistance in
1078 European field populations of *Tetranychus urticae*. Pest Manag Sci. 2020;76: 2569–2581.
1079 doi:10.1002/ps.5831

1080 51. Wybouw N, Kosterlitz O, Kurlovs AH, Bajda S, Greenhalgh R, Snoeck S, et al. Long-
1081 term population studies uncover the genome structure and genetic basis of xenobiotic and
1082 host plant adaptation in the herbivore *Tetranychus urticae*. Genetics. 2019;211: 1409–
1083 1427. doi:10.1534/genetics.118.301803

1084 52. Snoeck S, Kurlovs AH, Bajda S, Feyereisen R, Greenhalgh R, Villacis-Perez E, et al.
1085 High-resolution QTL mapping in *Tetranychus urticae* reveals acaricide-specific responses
1086 and common target-site resistance after selection by different METI-I acaricides. Insect
1087 Biochem Mol Biol. 2019;110: 19–33. doi:10.1016/j.ibmb.2019.04.011

1088 53. Fotoukkiaii SM, Wybouw N, Kurlovs AH, Tsakireli D, Pergantis SA, Clark RM, et al.
1089 High-resolution genetic mapping reveals *cis*-regulatory and copy number variation in loci
1090 associated with cytochrome P450-mediated detoxification in a generalist arthropod pest.
1091 PLoS Genet. 2021;17: e1009422. doi:10.1371/journal.pgen.1009422

1092 54. Villacis-Perez E, Snoeck S, Kurlovs AH, Clark RM, Breeuwer JAJ, Van Leeuwen T.
1093 Adaptive divergence and post-zygotic barriers to gene flow between sympatric
1094 populations of a herbivorous mite. Commun Biol. 2021;4: 853. doi:10.1038/s42003-021-
1095 02380-y

1096 55. De Beer B, Villacis-Perez E, Khalighi M, Saalwaechter C, Vandenhole M, Jonckheere W,
1097 et al. QTL mapping suggests that both cytochrome P450-mediated detoxification and
1098 target-site resistance are involved in fenbutatin oxide resistance in *Tetranychus urticae*.
1099 Insect Biochem Mol Biol. 2022; 103757. doi:10.1016/j.ibmb.2022.103757

1100 56. Bajda S, Dermauw W, Panteleri R, Sugimoto N, Douris V, Tirry L, et al. A mutation in
1101 the PSST homologue of complex I (NADH:ubiquinone oxidoreductase) from *Tetranychus*
1102 *urticae* is associated with resistance to METI acaricides. Insect Biochem Mol Biol.
1103 2017;80: 79–90. doi:10.1016/j.ibmb.2016.11.010

1104 57. Dermauw W, Ilias A, Riga M, Tsagkarakou A, Grbić M, Tirry L, et al. The cys-loop
1105 ligand-gated ion channel gene family of *Tetranychus urticae*: Implications for acaricide
1106 toxicology and a novel mutation associated with abamectin resistance. Insect Biochem
1107 Mol Biol. 2012;42: 455–465. doi:10.1016/j.ibmb.2012.03.002

1108 58. Hubert J, Nesvorna M, Kamler M, Kopecky J, Tyl J, Titera D, et al. Point mutations in the
1109 sodium channel gene conferring tau-fluvalinate resistance in *Varroa destructor*: point
1110 mutations in *VmNa*. Pest Manag Sci. 2014;70: 889–894. doi:10.1002/ps.3679

1111 59. González-Cabrera J, Rodríguez-Vargas S, Davies TGE, Field LM, Schmehl D, Ellis JD, et
1112 al. Novel mutations in the voltage-gated sodium channel of pyrethroid-resistant *Varroa*
1113 *destructor* populations from the Southeastern USA. PLoS One. 2016;11: e0155332.
1114 doi:10.1371/journal.pone.0155332

1115 60. Vlogiannitis S, Jonckheere W, Laget D, de Graaf DC, Vontas J, Van Leeuwen T.
1116 Pyrethroid target-site resistance mutations in populations of the honey bee parasite *Varroa*
1117 *destructor* (Acari: Varroidae) from Flanders, Belgium. Exp Appl Acarol. 2021;85: 205–
1118 221. doi:10.1007/s10493-021-00665-9

1119 61. Van Leeuwen T, Dermauw W, Mavridis K, Vontas J. Significance and interpretation of
1120 molecular diagnostics for insecticide resistance management of agricultural pests. Curr
1121 Opin Insect Sci. 2020;39: 69–76. doi:10.1016/j.cois.2020.03.006

1122 62. Xue W, Lu X, Mavridis K, Vontas J, Jonckheere W, Van Leeuwen T. The H92R
1123 substitution in PSST is a reliable diagnostic biomarker for predicting resistance to
1124 mitochondrial electron transport inhibitors of complex I in European populations of
1125 *Tetranychus urticae*. Pest Manag Sci. 2022; ps.7007. doi:10.1002/ps.7007

1126 63. Riga M, Bajda S, Themistokleous C, Papadaki S, Palzewicz M, Dermauw W, et al. The
1127 relative contribution of target-site mutations in complex acaricide resistant phenotypes as
1128 assessed by marker assisted backcrossing in *Tetranychus urticae*. Sci Rep. 2017;7.
1129 doi:10.1038/s41598-017-09054-y

1130 64. Van Leeuwen T, Demaeght P, Osborne EJ, Dermauw W, Gohlke S, Nauen R, et al.
1131 Population bulk segregant mapping uncovers resistance mutations and the mode of action
1132 of a chitin synthesis inhibitor in arthropods. Proc Natl Acad Sci USA. 2012;109: 4407–
1133 4412. doi:10.1073/pnas.1200068109

1134 65. Demaeght P, Osborne EJ, Odman-Naresh J, Grbić M, Nauen R, Merzendorfer H, et al.
1135 High resolution genetic mapping uncovers chitin synthase-1 as the target-site of the
1136 structurally diverse mite growth inhibitors clofentezine, hexythiazox and etoxazole in
1137 *Tetranychus urticae*. Insect Biochem Mol Biol. 2014;51: 52–61.
1138 doi:10.1016/j.ibmb.2014.05.004

1139 66. Rioja C, Zhurov V, Bruinsma K, Grbic M, Grbic V. Plant-herbivore interactions: a case of
1140 an extreme generalist, the two-spotted spider mite *Tetranychus urticae*. Mol Plant Microbe
1141 Interact. 2017;30: 935–945. doi:10.1094/MPMI-07-17-0168-CR

1142 67. Demaeght P, Dermauw W, Tsakireli D, Khajehali J, Nauen R, Tirry L, et al. Molecular
1143 analysis of resistance to acaricidal spirocyclic tetronic acids in *Tetranychus urticae*:
1144 CYP392E10 metabolizes spirodiclofen, but not its corresponding enol. Insect Biochem
1145 Mol Biol. 2013;43: 544–554. doi:10.1016/j.ibmb.2013.03.007

1146 68. Riga M, Tsakireli D, Ilias A, Morou E, Myridakis A, Stephanou EG, et al. Abamectin is
1147 metabolized by CYP392A16, a cytochrome P450 associated with high levels of acaricide
1148 resistance in *Tetranychus urticae*. Insect Biochem Mol Biol. 2014;46: 43–53.
1149 doi:10.1016/j.ibmb.2014.01.006

1150 69. Papapostolou KM, Riga M, Samantsidis G-R, Skoufa E, Balabanidou V, Van Leeuwen T,
1151 et al. Over-expression in *cis* of the midgut P450 CYP392A16 contributes to abamectin
1152 resistance in *Tetranychus urticae*. Insect Biochem Mol Biol. 2022;142: 103709.
1153 doi:10.1016/j.ibmb.2021.103709

1154 70. Helle W, Pieterse AH. Genetic affinities between adjacent populations of spider mites
1155 (*Tetranychus urticae* Koch). Entomol Exp Appl. 1965;8: 305–308. doi:10.1111/j.1570-
1156 7458.1965.tb00866.x

1157 71. Navajas M, Tsagkarakov A, Lagnel J, Perrot-Minnot M-J. Genetic differentiation in
1158 *Tetranychus urticae* (Acari: Tetranychidae): polymorphism, host races or sibling species?
1159 Exp Appl Acarol. 2000;24: 365–376. doi:10.1023/A:1006432604611

1160 72. Cruz MA, Magalhães S, Sucena É, Zélé F. *Wolbachia* and host intrinsic reproductive
1161 barriers contribute additively to postmating isolation in spider mites. Evolution. 2021;75:
1162 2085–2101. doi:10.1111/evo.14286

1163 73. Wu TD, Nacu S. Fast and SNP-tolerant detection of complex variants and splicing in short
1164 reads. Bioinformatics. 2010;26: 873–881. doi:10.1093/bioinformatics/btq057

1165 74. Wu TD, Reeder J, Lawrence M, Becker G, Brauer MJ. GMAP and GSNAP for genomic
1166 sequence alignment: enhancements to speed, accuracy, and functionality. In: Mathé E,
1167 Davis S, editors. Statistical Genomics. New York, NY: Springer New York; 2016. pp.
1168 283–334. doi:10.1007/978-1-4939-3578-9_15

1169 75. Fellous S, Angot G, Orsucci M, Migeon A, Auger P, Olivieri I, et al. Combining
1170 experimental evolution and field population assays to study the evolution of host range
1171 breadth. J Evol Biol. 2014;27: 911–919. doi:10.1111/jeb.12362

1172 76. Springer NM, Stupar RM. Allele-specific expression patterns reveal biases and embryo-
1173 specific parent-of-origin effects in hybrid maize. Plant Cell. 2007;19: 2391–2402.
1174 doi:10.1105/tpc.107.052258

1175 77. Villacis-Perez E, Alba JM, Cotte J, van Loon Z, Breeuwer JAJ, Van Leeuwen T.
1176 Interactions with plant defences isolate sympatric populations of an herbivorous mite.
1177 Front Ecol Evol. 2022;10: 819894. doi:10.3389/fevo.2022.819894

1178 78. Gould BA, Chen Y, Lowry DB. Gene regulatory divergence between locally adapted
1179 ecotypes in their native habitats. Mol Ecol. 2018;27: 4174–4188. doi:10.1111/mec.14852

1180 79. Cooper TF, Rozen DE, Lenski RE. Parallel changes in gene expression after 20,000
1181 generations of evolution in *Escherichia coli*. Proc Natl Acad Sci USA. 2003;100: 1072–
1182 1077. doi:10.1073/pnas.0334340100

1183 80. Stern DL, Orgogozo V. Is genetic evolution predictable? Science. 2009;323: 746–751.
1184 doi:10.1126/science.1158997

1185 81. Smith LB, Tyagi R, Kasai S, Scott JG. CYP-mediated permethrin resistance in *Aedes*
1186 *aegypti* and evidence for *trans*-regulation. Foster GM, editor. PLoS Negl Trop Dis.
1187 2018;12: e0006933. doi:10.1371/journal.pntd.0006933

1188 82. Duveau F, Zande PV, Metzger BPH, Diaz CJ, Walker EA, Tryban S, et al. Mutational
1189 sources of *trans*- regulatory variation affecting gene expression in *Saccharomyces*
1190 *cerevisiae*. Elife. 2021. doi:10.7554/eLife.67806

1191 83. King-Jones K, Horner MA, Lam G, Thummel CS. The DHR96 nuclear receptor regulates
1192 xenobiotic responses in *Drosophila*. Cell Metab. 2006;4: 37–48.
1193 doi:10.1016/j.cmet.2006.06.006

1194 84. Pascussi J-M, Gerbal-Chaloin S, Duret C, Daujat-Chavanieu M, Vilarem M-J, Maurel P.
1195 The tangle of nuclear receptors that controls xenobiotic metabolism and transport:
1196 crosstalk and consequences. Annu Rev Pharmacol Toxicol. 2008;48: 1–32.
1197 doi:10.1146/annurev.pharmtox.47.120505.105349

1198 85. Riga M, Myridakis A, Tsakireli D, Morou E, Stephanou EG, Nauen R, et al. Functional
1199 characterization of the *Tetranychus urticae* CYP392A11, a cytochrome P450 that
1200 hydroxylates the METI acaricides cyenopyrafen and fenpyroximate. Insect Biochem Mol
1201 Biol. 2015;65: 91–99. doi:10.1016/j.ibmb.2015.09.004

1202 86. Wilding CS, Smith I, Lynd A, Yawson AE, Weetman D, Paine MJI, et al. A *cis*-regulatory
1203 sequence driving metabolic insecticide resistance in mosquitoes: functional
1204 characterisation and signatures of selection. Insect Biochem Mol Biol. 2012;42: 699–707.
1205 doi:10.1016/j.ibmb.2012.06.003

1206 87. Pang R, Li Y, Dong Y, Liang Z, Zhang Y, Zhang W. Identification of promoter
1207 polymorphisms in the cytochrome P450 *CYP6AY1* linked with insecticide resistance in the
1208 brown planthopper, *Nilaparvata lugens*. Insect Mol Biol. 2014;23: 768–778.
1209 doi:10.1111/imb.12121

1210 88. Daborn PJ, Yen JL, Bogwitz MR, Le Goff G, Feil E, Jeffers S, et al. A single P450 allele
1211 associated with insecticide resistance in *Drosophila*. Science. 2002;297: 2253–2256.
1212 doi:10.1126/science.1074170

1213 89. Sayyed AH, Wright DJ. Cross-resistance and inheritance of resistance to *Bacillus*
1214 *thuringiensis* toxin Cry1Ac in diamondback moth (*Plutella xylostella* L) from lowland
1215 Malaysia. Pest Manag Sci. 2001;57: 413–421. doi:10.1002/ps.313

1216 90. Wang YH, Liu XG, Zhu YC, Wu SG, Li SY, Chen WM, et al. Inheritance mode and
1217 realized heritability of resistance to imidacloprid in the brown planthopper, *Nilaparvata*
1218 *lugens* (Stål) (Homoptera: Delphacidae). Pest Manag Sci. 2009;65: 629–634.
1219 doi:10.1002/ps.1720

1220 91. Diptaningsari D, Trisyono YA, Purwantoro A, Wijonarko A. Inheritance and realized
1221 heritability of resistance to imidacloprid in the brown planthopper, *Nilaparvata lugens*
1222 (Hemiptera: Delphacidae), from Indonesia. J Econ Entomol. 2019;112: 1831–1837.
1223 doi:10.1093/jee/toz090

1224 92. Mansoor MM, Shad SA. Methoxyfenozide tolerance in *Chrysoperla carnea*: inheritance,
1225 dominance and preliminary detoxification mechanisms. PLoS One. 2022;17: e0265304.
1226 doi:10.1371/journal.pone.0265304

1227 93. LeOra. POLO-Plus 1.0 Probit and Logit Analysis. Petaluma: LeOra Software; 2006.

1228 94. Robertson JL, Savin NE, Savin NE, Preisler HK. Bioassays with arthropods. 2nd ed. CRC
1229 Press; 2007. doi:10.1201/9781420004045

1230 95. R Core Team. R: A language and environment for statistical computing. Vienna, Austria:
1231 R Foundation for Statistical Computing; 2020. Available: https://www.R-project.org/

1232 96. Li H. Aligning sequence reads, clone sequences and assembly contigs with BWA-MEM.
1233 arXiv:13033997 [q-bio]. 2013. Available: http://arxiv.org/abs/1303.3997

1234 97. Li H, Handsaker B, Wysoker A, Fennell T, Ruan J, Homer N, et al. The Sequence
1235 Alignment/Map format and SAMtools. Bioinformatics. 2009;25: 2078–2079.
1236 doi:10.1093/bioinformatics/btp352

1237 98. McKenna A, Hanna M, Banks E, Sivachenko A, Cibulskis K, Kernytsky A, et al. The
1238 Genome Analysis Toolkit: a MapReduce framework for analyzing next-generation DNA
1239 sequencing data. Genome Res. 2010;20: 1297–1303. doi:10.1101/gr.107524.110

1240 99. DePristo MA, Banks E, Poplin R, Garimella KV, Maguire JR, Hartl C, et al. A framework
1241 for variation discovery and genotyping using next-generation DNA sequencing data. Nat
1242 Genet. 2011;43: 491–498. doi:10.1038/ng.806

1243 100. Cingolani P, Platts A, Wang LL, Coon M, Nguyen T, Wang L, et al. A program for
1244 annotating and predicting the effects of single nucleotide polymorphisms, SnpEff: SNPs in
1245 the genome of *Drosophila melanogaster* strain w ^{1118} ; iso-2; iso-3. Fly. 2012;6: 80–92.
1246 doi:10.4161/fly.19695

1247 101. Sterck L, Billiau K, Abeel T, Rouzé P, Van de Peer Y. ORCAE: online resource for
1248 community annotation of eukaryotes. Nat Methods. 2012;9: 1041–1041.
1249 doi:10.1038/nmeth.2242

1250 102. Zheng X, Levine D, Shen J, Gogarten SM, Laurie C, Weir BS. A high-performance
1251 computing toolset for relatedness and principal component analysis of SNP data.
1252 Bioinformatics. 2012;28: 3326–3328. doi:10.1093/bioinformatics/bts606

1253 103. Zheng X, Gogarten SM, Lawrence M, Stilp A, Conomos MP, Weir BS, et al. SeqArray—a
1254 storage-efficient high-performance data format for WGS variant calls. Bioinformatics.
1255 2017;33: 2251–2257. doi:10.1093/bioinformatics/btx145

1256 104. Cowles CR, Hirschhorn JN, Altshuler D, Lander ES. Detection of regulatory variation in
1257 mouse genes. Nat Genet. 2002;32: 432–437. doi:10.1038/ng992

1258 105. Anders S, Pyl PT, Huber W. HTSeq—a Python framework to work with high-throughput
1259 sequencing data. Bioinformatics. 2015;31: 166–169. doi:10.1093/bioinformatics/btu638

1260 106. Love MI, Huber W, Anders S. Moderated estimation of fold change and dispersion for
1261 RNA-seq data with DESeq2. Genome Biol. 2014;15: 1–21. doi:10.1186/s13059-014-
1262 0550-8

1263 107. Cock PJA, Antao T, Chang JT, Chapman BA, Cox CJ, Dalke A, et al. Biopython: freely
1264 available Python tools for computational molecular biology and bioinformatics.
1265 Bioinformatics. 2009;25: 1422–1423. doi:10.1093/bioinformatics/btp163

1266 108. Stephens M. False discovery rates: a new deal. Biostatistics. 2017;18: 275–294.
1267 doi:10.1093/biostatistics/kxw041

1268 109. Stone BF. A formula for determining degree of dominance in cases of monofactorial
1269 inheritance of resistance to chemicals. Bull World Health Organ. 1968;38: 325–326.

1270 110. Jones P, Binns D, Chang H-Y, Fraser M, Li W, McAnulla C, et al. InterProScan 5:
1271 genome-scale protein function classification. Bioinformatics. 2014;30: 1236.
1272 doi:10.1093/bioinformatics/btu031

1273 111. Edgar RC. MUSCLE: multiple sequence alignment with high accuracy and high
1274 throughput. Nucleic Acids Res. 2004;32: 1792–1797. doi:10.1093/nar/gkh340

1275 112. Huerta-Cepas J, Dopazo J, Gabaldón T. ETE: a python environment for tree exploration.
1276 BMC Bioinformatics. 2010;11: 24. doi:10.1186/1471-2105-11-24

1277 113. Hunter JD. Matplotlib: a 2D graphics environment. Comput Sci Eng. 2007;9: 90–95.
1278 doi:10.1109/MCSE.2007.55

1279

1280 # Figures and legends

1281 **Fig 1**. **Genetic and gene expression relatedness among five inbred *T. urticae* strains.** (A) A principal
1282 component (PC) analysis based on genetic variation (SNPs) shows relatedness among the five strains, as
1283 indicated by points with attending inbred strain names. (B) A PC analysis based on transcriptome profiles
1284 shows the similarities among the five strains and the F1 hybrids developed from crosses of four strains
1285 (ROS-ITi, JP-RRi, MAR-ABi, and MR-VPi) to a common parent (SOL-BEi). For F1 samples, labeling is
1286 based on the parent that varies (i.e., the non-SOL-BEi parent). Transcriptome data was collected from 4-7
1287 day-old adult females, and each dot represents a biological replicate (4-5 replicates were used for each
1288 genotype). For both panels, PC1 and PC2 are indicated on the x- and y-axes, respectively (the percent of
1289 variance explained by each PC is given in parenthesis).

1290

1291 **Fig 2**. **Resistance phenotypes of inbred strains to twelve compounds and their performance on host**
1292 **plants.** (A) A heatmap showing resistance of five inbred *T. urticae* strains (top) to 12 acaricide compounds
1293 (left; IRAC pesticide classes are indicated at right). Log-transformed resistance ratios (RRs) were calculated
1294 based on the least resistant strain (scale, bottom). Within each cell, LC_{50} values (mg L^{-1}) are shown above
1295 the log-transformed RRs (in parentheses). For a given compound, strains for which LC_{50} values are not
1296 significantly different from each other have the same number of plus signs (indicated between LC_{50} values
1297 and the log-transformed RR values); the number of plus signs negatively correlates with resistance level
1298 (i.e., strains with a single plus sign have the highest LC_{50} values for a given acaricide, while strains with
1299 the highest number of plus signs have the lowest). By strain and compound, an asterisk (top right corner)
1300 denotes the presence of established target-site resistance mutations in *T. urticae* (S2 Table); the presence
1301 of target site mutations studied in other species, but not validated in *T. urticae,* are denoted by a question
1302 mark (bifenthrin only). All phenotypic data is from the current study, excepting that for fenbutatin oxide in
1303 strains SOL-BEi and MAR-ABi, which was reported previously by De Beer et al. [55]. (B) The total number
1304 of eggs laid by sets of ten mites (each a single replicate) on the adaxial side of bean, cucumber, tomato,

1305 prune and potato leaf disks over a 3-day period is as indicated (legend, lower right). The data is displayed
1306 using boxplots with an overlay of data points (the number of replicates is given in parentheses). *P*-values
1307 (*p*) displayed are from an ANOVA; all significant pairwise differences among strains by host plant are
1308 indicated by asterisks ($p \leq 0.05$: *, $p \leq 0.01$: **, $p \leq 0.001$: ***, and $p \leq 0.0001$: ****, with post-hoc Tukey
1309 test to adjust for multiple testing).
1310
1311 **Fig 3. Regulatory modes associated with gene expression variation in comparisons of parental strains**
1312 **and allele-specific expression in F1s**. (A-D) For the comparisons of ROS-ITi (A), JP-RRi (B), MAR-ABi
1313 (C), and MR-VPi (D) to SOL-BEi, scatter plots show $\log_2$ fold change ($\log_2$FC) for genes with assigned
1314 genetic modes of control between the respective parents (y-axis) versus respective $\log_2$FC for allele-specific
1315 expression in F1s (x-axis) (for this analysis, genes assigned to conserved or ambiguous modes are not
1316 shown; $\log_2$FC values falling outside the plotting scale of -10 to 10 were rescaled to these limits for
1317 plotting). Each point represents a single gene, with color coding by *cis*, *trans*, synergism, antagonism, and
1318 compensatory mode of genetic control as indicated (see insets for color codes and respective gene numbers;
1319 *n*, total sample size, upper left). (E-H) Respective plots for panels A-D except that only genes in the
1320 detoxification/host/peptidase (D+H+P) gene set are plotted, and with selection for genes with moderate to
1321 large absolute value of $\log_2$FC (> 1) along one or more axes. Different symbols and outline colors denote
1322 membership in the various D+H+P gene families or gene set classifications (see legends to the right of each
1323 panel). The interiors of plotting symbols are color coded by the regulatory categories as indicated in the
1324 insets (*n*, total sample size, upper left). For each gene family or for host genes, in the legends the three
1325 numbers in parentheses represent (*i*) the number of genes shown in each panel with *cis*, *trans*, synergism,
1326 antagonism, and compensatory mode assignments for which $|\log_2\text{FC}| > 1$, (*ii*) genes with the same selection
1327 criteria except with no $\log_2$FC cutoff applied, out of (*iii*) the total number of genes for which any mode of
1328 genetic control could be assigned (including conserved and ambiguous; see also S2 Fig). The data upon
1329 which this figure is based are provided in S4 Table.
1330

1331 **Fig 4. Composition of genetic control categories stratified by magnitude of parental expression fold**
1332 **change differences.** (A) For all genes for which *cis*, *trans*, synergism, antagonism or compensatory modes
1333 of expression control (legend, top right) could be assigned in pairwise strain comparisons, stacked barplots
1334 show respective percentages stratified by increasing absolute value of $\log_2$ fold change ($|\log_2 FC|$) bins for
1335 parental expression differences (denoted beneath each subpanel; the four genotypic comparisons, as well
1336 as respective sample sizes, *n*, are indicated above each subpanel). (B) Same as for panel (A) except for the
1337 subset of genes in the detoxification/host/peptidase (D+H+P) gene set. The data upon which this figure is
1338 based are provided in S4 Table.
1339
1340 **Fig 5. The contribution of *cis* and *trans* effects for CYP gene expression variation among pairwise**
1341 **strain comparisons.** A heatmap (center right; scale, bottom left) shows $\log_2$ fold change ($\log_2 FC$) values
1342 for CYPs between parents (a combination of *cis* and *trans* effects, denoted "*cis* + *trans*"), for ASE in F1s
1343 (which correspond to *cis* effects only, denoted *cis*), and for the *trans* contribution as inferred from the *cis* +
1344 *trans* and *cis* $\log_2 FC$ values (see Methods). These groupings are as indicated at the top, and the pairs of
1345 strains for the four comparisons are indicated at bottom (exact $\log_2 FC$ values are given internal to each cell,
1346 and if significant, an asterisk is used; see also S4 Table). Genes with $\log_2 FC > 1$ attributed to *trans* in at
1347 least one of the comparisons are in bold, and genes with $\log_2 FC < -1$ attributed to *trans* in at least one of
1348 the comparisons are underlined. CYP gene names are given to the left, and are ordered based on a neighbor-
1349 joining phylogenetic tree (far left). CYP clan membership is indicated at the far right, with branches in the
1350 tree also color-coded respectively. For inclusion of a CYP in the analysis, a genetic mode of control had to
1351 be assigned in at least one comparison. Where information for a gene was not available in a specific
1352 genotypic comparison (see Methods), cells are colored in gray.
1353
1354 **Fig 6**. **Inheritance of gene expression and its association with regulatory categories for gene**
1355 **expression variation.** (A-B) Stacked barplots display the composition of each inheritance mode for
1356 comparisons of four strains (ROS-ITi, JP-RRi, MAR-ABi, and MR-VPi, indicated as P1, see labels at

1357 bottom) to a common parent (SOL-BEi, indicated as P2) for all genes (A) and for those in the
1358 detoxification/host/peptidase (D+H+P) gene set (B). The following inheritance classifications were made:
1359 (*i*) additive, where that of F1 equals the average expression of the respective parents, (*ii*) dominant, where
1360 that of the F1 equals expression of one parent (the direction of dominance is as indicated in the legend at
1361 the far left), and (*iii*) transgressive, for which F1 values are outside the range of the parents (the direction
1362 of transgression is defined as either up or down with respect to the parental range). The number of genes
1363 (y-axis) for P1>P2 (above 0) and P1<P2 (below 0) are as indicated above or below the bars in the plot, with
1364 coloring of stacked bars denoting inheritance classifications (see legend, far right; within the stacked bar
1365 plots, exact percentages are given for modes > 5%). In panels A and B, transgressive inheritance for which
1366 P1=P2 (no expression difference between parents) is not indicated. (C) Line plot displaying the relative
1367 proportions of additive and dominant inheritance modes (y-axis) stratified by absolute values of $\log_2$ fold
1368 change in comparisons between parents ($|\log_2(P1/P2)|$, x-axis). The different line types represent the four
1369 comparisons, and different colors denote additive or dominant modes (see legend at right). (D) The
1370 association between each combination of mode of genetic control (*cis*, *trans,* synergism, and antagonism)
1371 and inheritance mode (additive, dominant, and transgressive). The significance of enrichment (blue) or
1372 depletion (red) is denoted using asterisks (Chi-square test of independence followed by Benjamini-
1373 Hochberg multiple test corrections; adjusted $p < 0.001$: ***; adjusted $p < 0.01$: **; adjusted $p < 0.05$: *).
1374 The data upon which this figure is based are provided in S7 Table.
1375

1376 # Supporting information

1377 **S1 Fig. Gene numbers for inclusion in assessing genetic mode of control of expression variation.** (A)
1378 A Venn diagram shows the number of intact+single copy genes available for potential assessment of genetic
1379 mode of control by comparison of strains ROS-ITi, JP-RRi, MAR-ABi, and MR-VPi to a single parent
1380 strain (SOL-BEi), and the overlap among the comparisons (for details, see Methods, and S3 Table). (B) A
1381 Venn diagram after panel (A) but indicating the number of genes in each comparison, and the overlap
1382 among comparisons, where an assignment of genetic mode of control could be made (categories *cis*, *trans*,
1383 synergism, antagonism, compensatory, conserved, and ambiguous). See S4 Table for the respective genes
1384 by comparison.

1385 **S2 Fig. The composition of genetic mode of gene expression control in pairwise strain comparisons**
1386 **by gene group.** For pairwise comparisons of each of ROS-ITi (A), JP-RRi (B), MAR-ABi (C), and MR-
1387 VPi (D) to SOL-BEi, the number of genes assigned into one of the seven genetic control categories is
1388 indicated above the stacked barplots (categories *cis*, *trans*, synergism, antagonism, compensatory,
1389 conserved, and ambiguous are as indicated by color in the stacks, see the legend at top). In each of panels
1390 A-D, classifications are shown for all genes in the left subpanel, and at right for genes in the
1391 detoxification/host/peptidase (D+H+P) gene set sorted by gene family or group (as in the case of host
1392 genes). The data upon which this figure is based are provided in S4 Table.

1393

1394 **S3 Fig. The contribution of *cis* and *trans* effects for dioxygenase gene expression variation among**
1395 **pairwise strain comparisons.** A heatmap (center right; scale, bottom left) shows $\log_2$ fold change ($\log_2$FC)
1396 values for dioxygenase (DOG) genes between parents (a combination of *cis* and *trans* effects, denoted "*cis*
1397 + *trans*"), for ASE in F1s (which correspond to *cis* effects only, denoted *cis*), and for the *trans* contribution
1398 as inferred from the *cis* + *trans* and *cis* $\log_2$FC values (see Methods). These groupings are as indicated at
1399 the top, and the pairs of strains for the four comparisons are indicated at bottom (exact $\log_2$FC values are
1400 given internal to each cell, and if significant, an asterisk is used; see also S4 Table). Genes are ordered

1401 based on a neighbor-joining phylogenetic tree as indicated on the left. For inclusion of a DOG in the
1402 analysis, a genetic mode of control had to have been assigned in at least one comparison. Where information
1403 for a gene was not available in a specific genotypic comparison, cells are colored in gray.
1404
1405 **S4 Fig. The contribution of *cis* and *trans* effects for lipocalin gene expression variation among**
1406 **pairwise strain comparisons.** A heatmap (center right; scale, bottom left) shows $\log_2$ fold change ($\log_2$FC)
1407 values for lipocalin genes between parents (a combination of *cis* and *trans* effects, denoted "*cis* + *trans*"),
1408 for ASE in F1s (which correspond to *cis* effects only, denoted *cis*), and for the *trans* contribution as inferred
1409 from the *cis* + *trans* and *cis* $\log_2$FC values (see Methods). These groupings are as indicated at the top, and
1410 the pairs of strains for the four comparisons are indicated at bottom (exact $\log_2$FC values are given internal
1411 to each cell, and if significant, an asterisk is used; see also S4 Table). Genes are ordered based on a neighbor-
1412 joining phylogenetic tree as indicated on the left. For inclusion of a lipocalin in the analysis, a genetic mode
1413 of control had to be assigned in at least one comparison. Where information for a gene was not available in
1414 a specific genotypic comparison, cells are colored in gray.
1415
1416 **S5 Fig. The contribution of *cis* and *trans* effects for short-chain dehydrogenase/reductase gene**
1417 **expression variation among pairwise strain comparisons.** A heatmap (center right; scale, bottom left)
1418 shows $\log_2$ fold change ($\log_2$FC) values for short-chain dehydrogenases/reductase (SDR) genes between
1419 parents (a combination of *cis* and *trans* effects, denoted "*cis* + *trans*"), for ASE in F1s (which correspond
1420 to *cis* effects only, denoted *cis*), and for the *trans* contribution as inferred from the *cis* + *trans* and *cis* $\log_2$FC
1421 values (see Methods). These groupings are as indicated at the top, and the pairs of strains for the four
1422 comparisons are indicated at bottom (exact $\log_2$FC values are given internal to each cell, and if significant,
1423 an asterisk is used; see also S4 Table). Genes are ordered based on a neighbor-joining phylogenetic tree as
1424 indicated on the left. For inclusion of a SDR in the analysis, a genetic mode of control had to be assigned
1425 in at least one comparison. Where information for a gene was not available in a specific genotypic
1426 comparison, cells are colored in gray.

1427

1428 **S1 Table. Chemical compounds used in the bioassays with concentration, corresponding IRAC**

1429 **group, mode of action (MoA) and time of mortality assessment**

1430

1431 **S2 Table. Target site mutations present by strain.**

1432

1433 **S3 Table. Putative intact+single copy genes in pairwise comparisons**

1434

1435 **S4 Table. Regulatory modes for gene expression variation in pairwise comparisons.**

1436

1437 **S5 Table. Genes in the detoxification/host/peptidase (D+H+P) gene set.**

1438

1439 **S6 Table. Enriched gene ontology (GO) terms for genes with extremes of *trans* genetic control.**

1440

1441 **S7 Table. Gene expression inheritance inferred in pairwise comparisons.**

1442

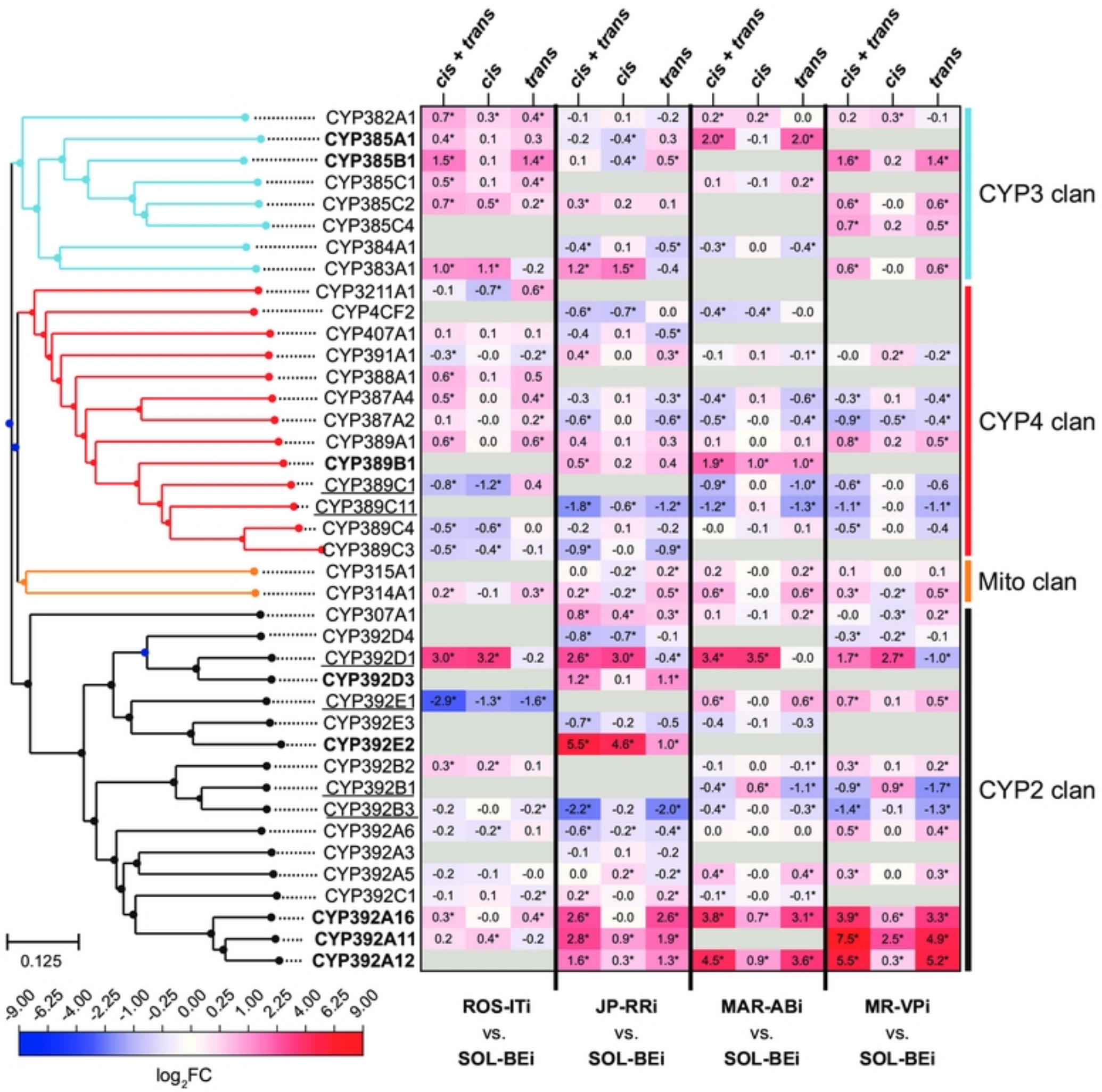
cis + trans
cis
trans
ROS-ITi vs. SOL-BEi
JP-RRi vs. SOL-BEi
MAR-ABi vs. SOL-BEi
MR-VPi vs. SOL-BEi
CYP382A1
CYP385A1
CYP385B1
CYP385C1
CYP385C2
CYP385C4
CYP384A1
CYP383A1
CYP3211A1
CYP4CF2
CYP407A1
CYP391A1
CYP388A1
CYP387A4
CYP387A2
CYP389A1
CYP389B1
CYP389C1
CYP389C11
CYP389C4
CYP389C3
CYP315A1
CYP314A1
CYP307A1
CYP392D4
CYP392D1
CYP392D3
CYP392E1
CYP392E3
CYP392E2
CYP392B2
CYP392B1
CYP392B3
CYP392A6
CYP392A3
CYP392A5
CYP392C1
CYP392A16
CYP392A11
CYP392A12
CYP3 clan
CYP4 clan
Mito clan
CYP2 clan
0.125
-9.00 -6.25 -4.00 -2.25 -1.00 -0.25 0.00 0.25 1.00 2.25 4.00 6.25 9.00
log2FC

Fig 5

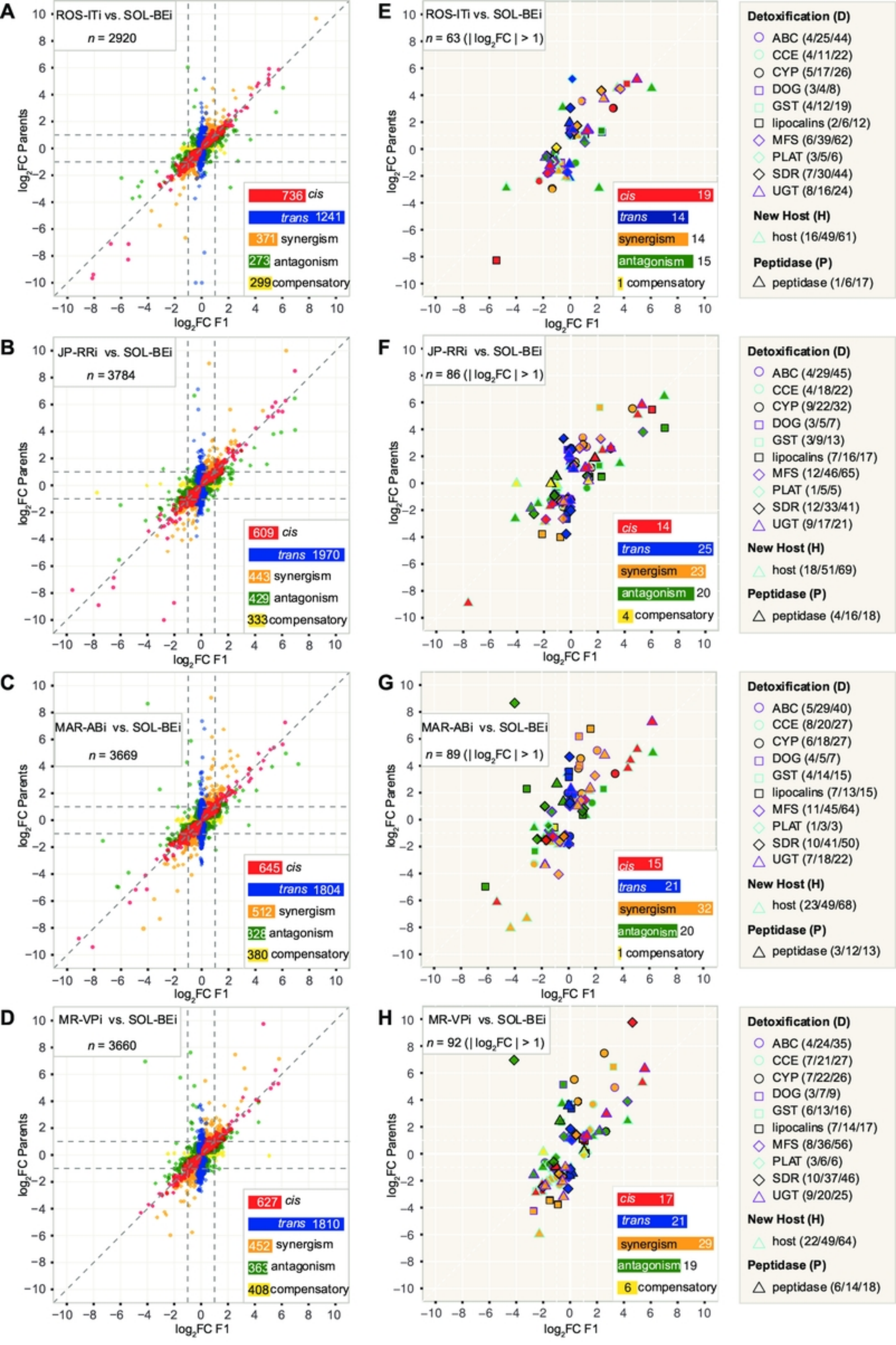
A
ROS-ITi vs. SOL-BEi
n = 2920
736 cis
trans 1241
371 synergism
273 antagonism
299 compensatory
B
JP-RRi vs. SOL-BEi
n = 3784
609 cis
trans 1970
443 synergism
429 antagonism
333 compensatory
C
MAR-ABi vs. SOL-BEi
n = 3669
645 cis
trans 1804
512 synergism
328 antagonism
380 compensatory
D
MR-VPi vs. SOL-BEi
n = 3660
627 cis
trans 1810
452 synergism
363 antagonism
408 compensatory
E
ROS-ITi vs. SOL-BEi
n = 63 (| log2FC | > 1)
cis 19
trans 14
synergism 14
antagonism 15
1 compensatory
F
JP-RRi vs. SOL-BEi
n = 86 (| log2FC | > 1)
cis 14
trans 25
synergism 23
antagonism 20
4 compensatory
G
MAR-ABi vs. SOL-BEi
n = 89 (| log2FC | > 1)
cis 15
trans 21
synergism 32
antagonism 20
1 compensatory
H
MR-VPi vs. SOL-BEi
n = 92 (| log2FC | > 1)
cis 17
trans 21
synergism 29
antagonism 19
6 compensatory
log2FC Parents
log2FC F1
Detoxification (D)
ABC (4/25/44)
CCE (4/11/22)
CYP (5/17/26)
DOG (3/4/8)
GST (4/12/19)
lipocalins (2/6/12)
MFS (6/39/62)
PLAT (3/5/6)
SDR (7/30/44)
UGT (8/16/24)
New Host (H)
host (16/49/61)
Peptidase (P)
peptidase (1/6/17)
Detoxification (D)
ABC (4/29/45)
CCE (4/18/22)
CYP (9/22/32)
DOG (3/5/7)
GST (3/9/13)
lipocalins (7/16/17)
MFS (12/46/65)
PLAT (1/5/5)
SDR (12/33/41)
UGT (9/17/21)
New Host (H)
host (18/51/69)
Peptidase (P)
peptidase (4/16/18)
Detoxification (D)
ABC (5/29/40)
CCE (8/20/27)
CYP (6/18/27)
DOG (4/5/7)
GST (4/14/15)
lipocalins (7/13/15)
MFS (11/45/64)
PLAT (1/3/3)
SDR (10/41/50)
UGT (7/18/22)
New Host (H)
host (23/49/68)
Peptidase (P)
peptidase (3/12/13)
Detoxification (D)
ABC (4/24/35)
CCE (7/21/27)
CYP (7/22/26)
DOG (3/7/9)
GST (6/13/16)
lipocalins (7/14/17)
MFS (8/36/56)
PLAT (3/6/6)
SDR (10/37/46)
UGT (9/20/25)
New Host (H)
host (22/49/64)
Peptidase (P)
peptidase (6/14/18)

Fig 3

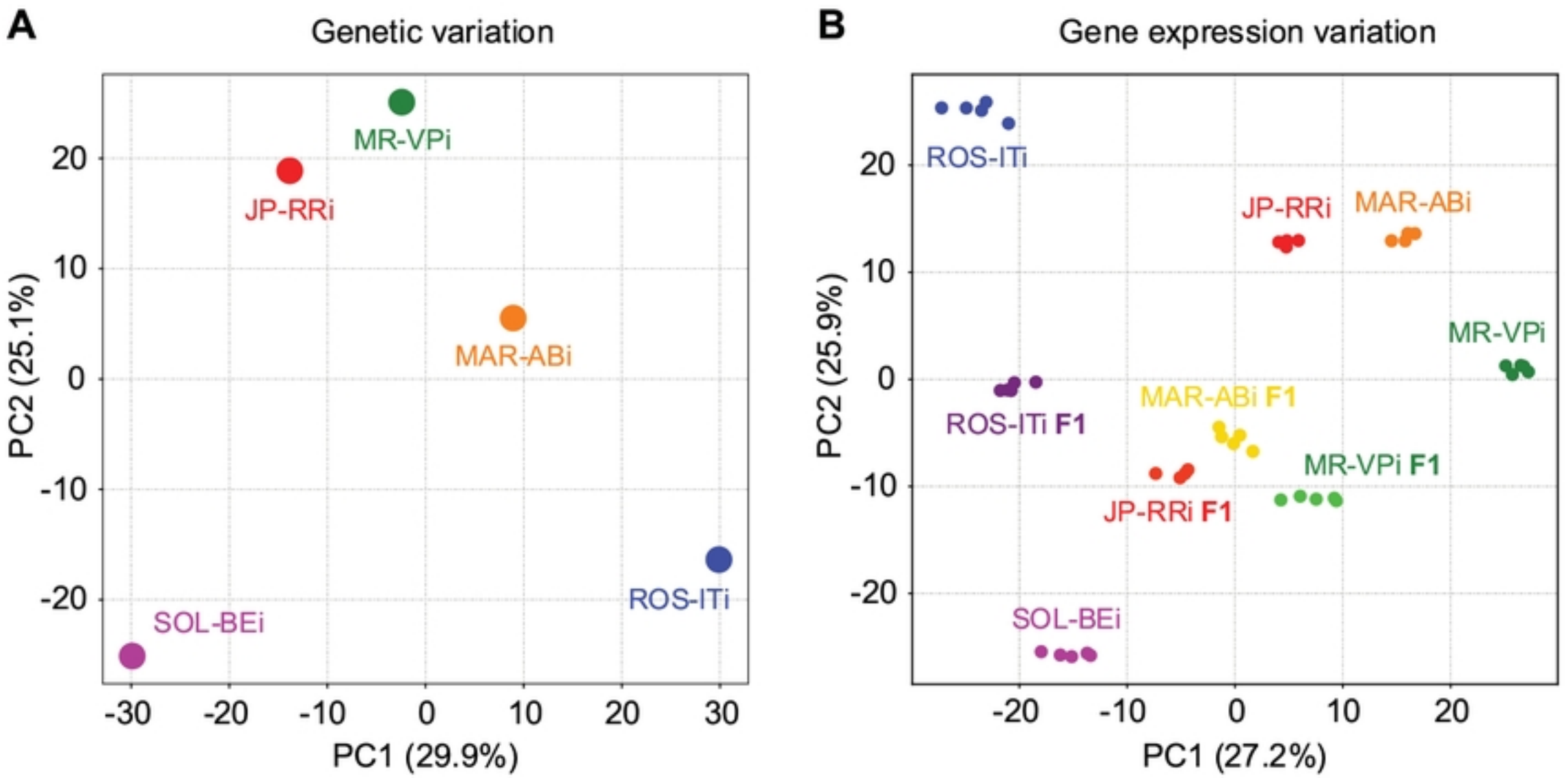
A
Genetic variation
MR-VPi
JP-RRi
MAR-ABi
ROS-ITi
SOL-BEi
PC2 (25.1%)
PC1 (29.9%)
20
10
0
-10
-20
-30
-20
-10
0
10
20
30
B
Gene expression variation
ROS-ITi
JP-RRi
MAR-ABi
MR-VPi
MAR-ABi F1
ROS-ITi F1
MR-VPi F1
JP-RRi F1
SOL-BEi
PC2 (25.9%)
PC1 (27.2%)
20
10
0
-10
-20
-20
-10
0
10
20

Fig 1

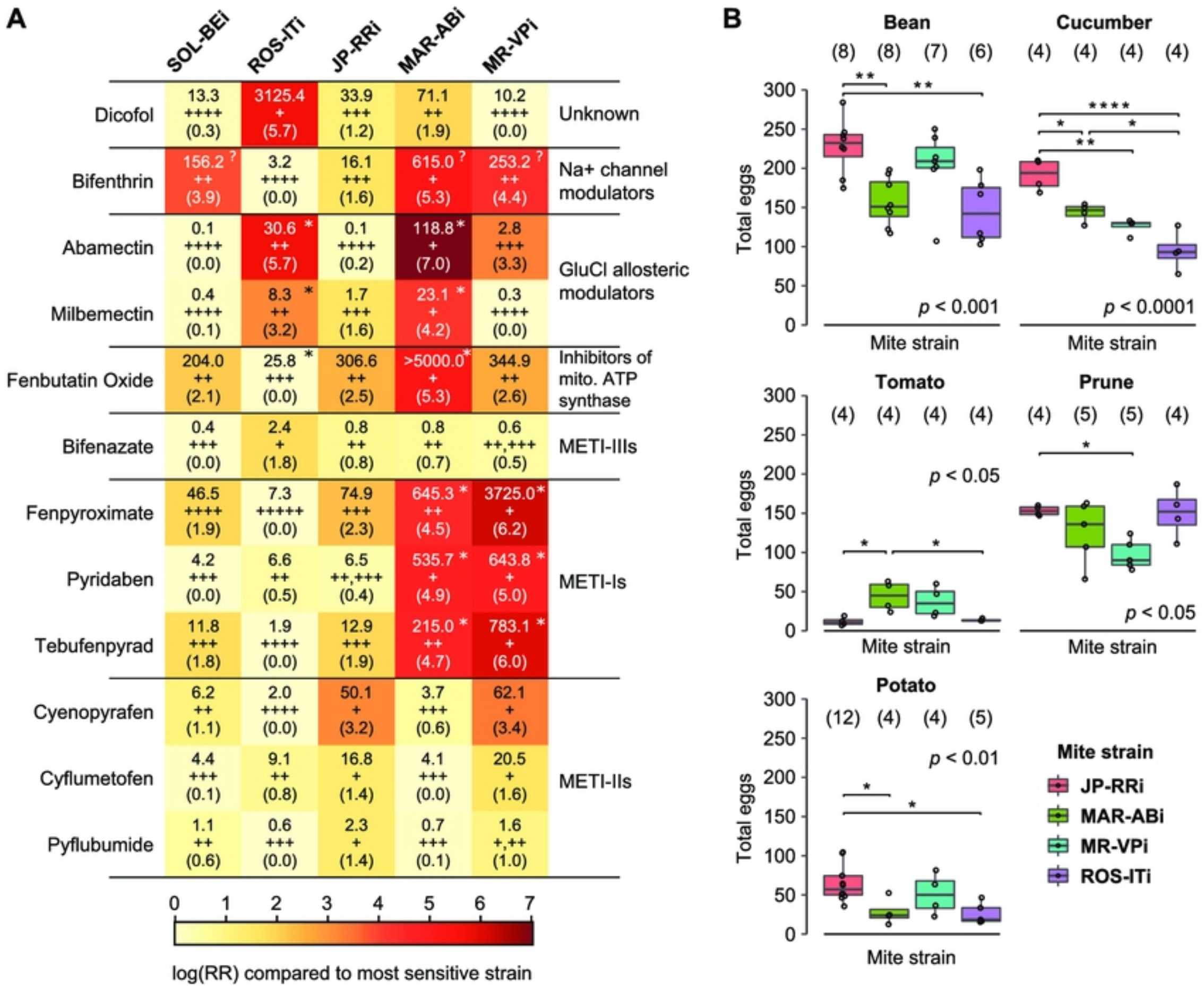
A
SOL-BEi
ROS-ITi
JP-RRi
MAR-ABi
MR-VPi
Dicofol
13.3 ++++ (0.3)
3125.4 + (5.7)
33.9 +++ (1.2)
71.1 ++ (1.9)
10.2 ++++ (0.0)
Unknown
Bifenthrin
156.2 ? ++ (3.9)
3.2 ++++ (0.0)
16.1 +++ (1.6)
615.0 ? + (5.3)
253.2 ? ++ (4.4)
Na+ channel modulators
Abamectin
0.1 ++++ (0.0)
30.6 * ++ (5.7)
0.1 ++++ (0.2)
118.8 * + (7.0)
2.8 +++ (3.3)
Milbemectin
0.4 ++++ (0.1)
8.3 * ++ (3.2)
1.7 +++ (1.6)
23.1 * + (4.2)
0.3 ++++ (0.0)
GluCl allosteric modulators
Fenbutatin Oxide
204.0 ++ (2.1)
25.8 * +++ (0.0)
306.6 ++ (2.5)
>5000.0 * + (5.3)
344.9 ++ (2.6)
Inhibitors of mito. ATP synthase
Bifenazate
0.4 +++ (0.0)
2.4 + (1.8)
0.8 ++ (0.8)
0.8 ++ (0.7)
0.6 ++,+++ (0.5)
METI-IIIs
Fenpyroximate
46.5 ++++ (1.9)
7.3 +++++ (0.0)
74.9 +++ (2.3)
645.3 * ++ (4.5)
3725.0 * + (6.2)
Pyridaben
4.2 +++ (0.0)
6.6 ++ (0.5)
6.5 ++,+++ (0.4)
535.7 * + (4.9)
643.8 * + (5.0)
Tebufenpyrad
11.8 +++ (1.8)
1.9 ++++ (0.0)
12.9 +++ (1.9)
215.0 * ++ (4.7)
783.1 * + (6.0)
METI-Is
Cyenopyrafen
6.2 ++ (1.1)
2.0 ++++ (0.0)
50.1 + (3.2)
3.7 +++ (0.6)
62.1 + (3.4)
Cyflumetofen
4.4 +++ (0.1)
9.1 ++ (0.8)
16.8 + (1.4)
4.1 +++ (0.0)
20.5 + (1.6)
Pyflubumide
1.1 ++ (0.6)
0.6 +++ (0.0)
2.3 + (1.4)
0.7 +++ (0.1)
1.6 +,++ (1.0)
METI-IIs
0 1 2 3 4 5 6 7
log(RR) compared to most sensitive strain
B
Bean
(8) (8) (7) (6)
Cucumber
(4) (4) (4) (4)
Total eggs
p < 0.001
p < 0.0001
Mite strain
Tomato
(4) (4) (4) (4)
Prune
(4) (5) (5) (4)
p < 0.05
p < 0.05
Potato
(12) (4) (4) (5)
p < 0.01
Mite strain
JP-RRi
MAR-ABi
MR-VPi
ROS-ITi

Fig 2

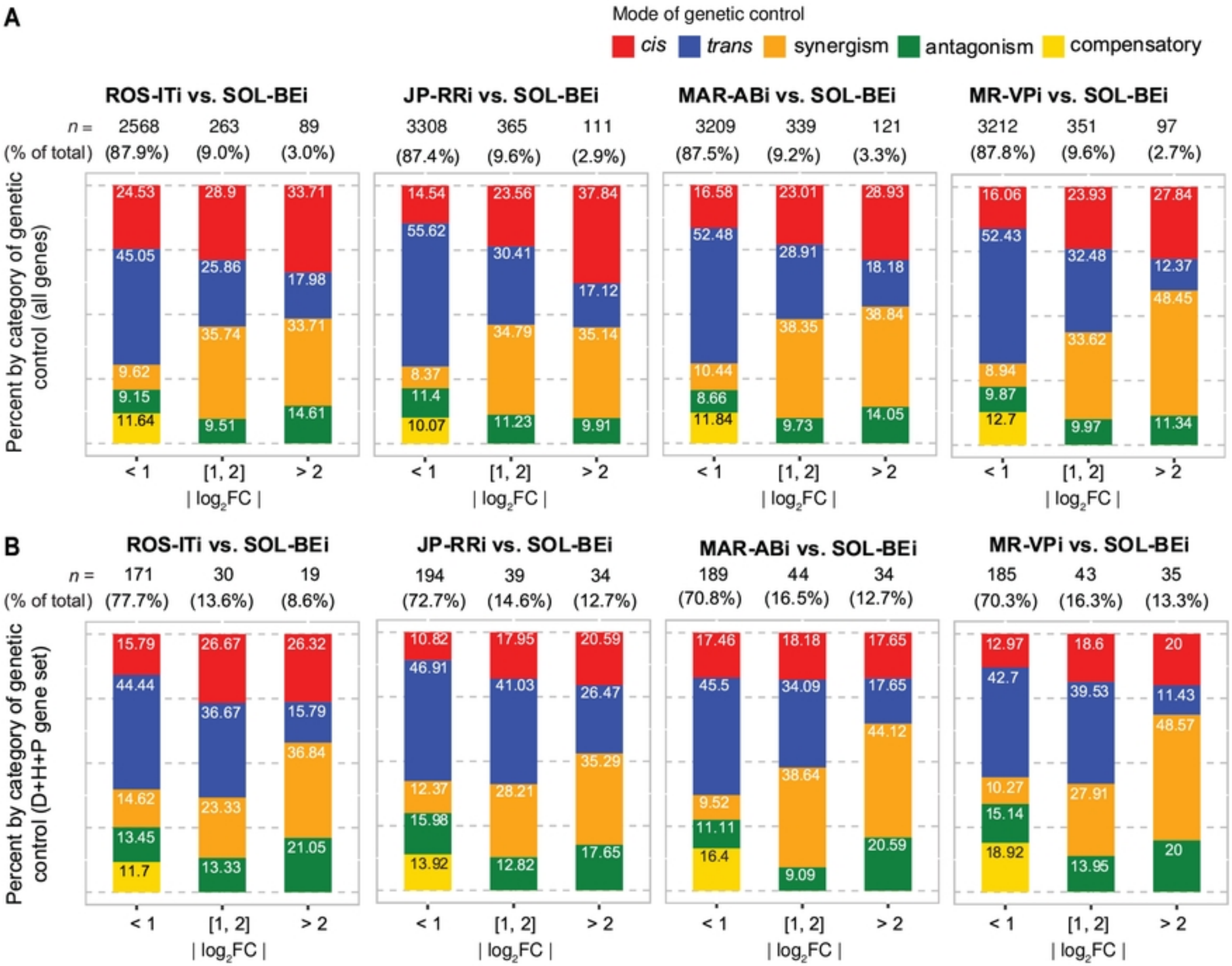
A
Mode of genetic control
cis
trans
synergism
antagonism
compensatory
ROS-ITi vs. SOL-BEi
JP-RRi vs. SOL-BEi
MAR-ABi vs. SOL-BEi
MR-VPi vs. SOL-BEi
n =
(% of total)
2568 (87.9%)
263 (9.0%)
89 (3.0%)
3308 (87.4%)
365 (9.6%)
111 (2.9%)
3209 (87.5%)
339 (9.2%)
121 (3.3%)
3212 (87.8%)
351 (9.6%)
97 (2.7%)
Percent by category of genetic control (all genes)
24.53
45.05
9.62
9.15
11.64
28.9
25.86
35.74
9.51
33.71
17.98
33.71
14.61
14.54
55.62
8.37
11.4
10.07
23.56
30.41
34.79
11.23
37.84
17.12
35.14
9.91
16.58
52.48
10.44
8.66
11.84
23.01
28.91
38.35
9.73
28.93
18.18
38.84
14.05
16.06
52.43
8.94
9.87
12.7
23.93
32.48
33.62
9.97
27.84
12.37
48.45
11.34
< 1
[1, 2]
> 2
| log2FC |
B
ROS-ITi vs. SOL-BEi
JP-RRi vs. SOL-BEi
MAR-ABi vs. SOL-BEi
MR-VPi vs. SOL-BEi
n =
(% of total)
171 (77.7%)
30 (13.6%)
19 (8.6%)
194 (72.7%)
39 (14.6%)
34 (12.7%)
189 (70.8%)
44 (16.5%)
34 (12.7%)
185 (70.3%)
43 (16.3%)
35 (13.3%)
Percent by category of genetic control (D+H+P gene set)
15.79
44.44
14.62
13.45
11.7
26.67
36.67
23.33
13.33
26.32
15.79
36.84
21.05
10.82
46.91
12.37
15.98
13.92
17.95
41.03
28.21
12.82
20.59
26.47
35.29
17.65
17.46
45.5
9.52
11.11
16.4
18.18
34.09
38.64
9.09
17.65
17.65
44.12
20.59
12.97
42.7
10.27
15.14
18.92
18.6
39.53
27.91
13.95
20
11.43
48.57
20
< 1
[1, 2]
> 2
| log2FC |

Fig 4

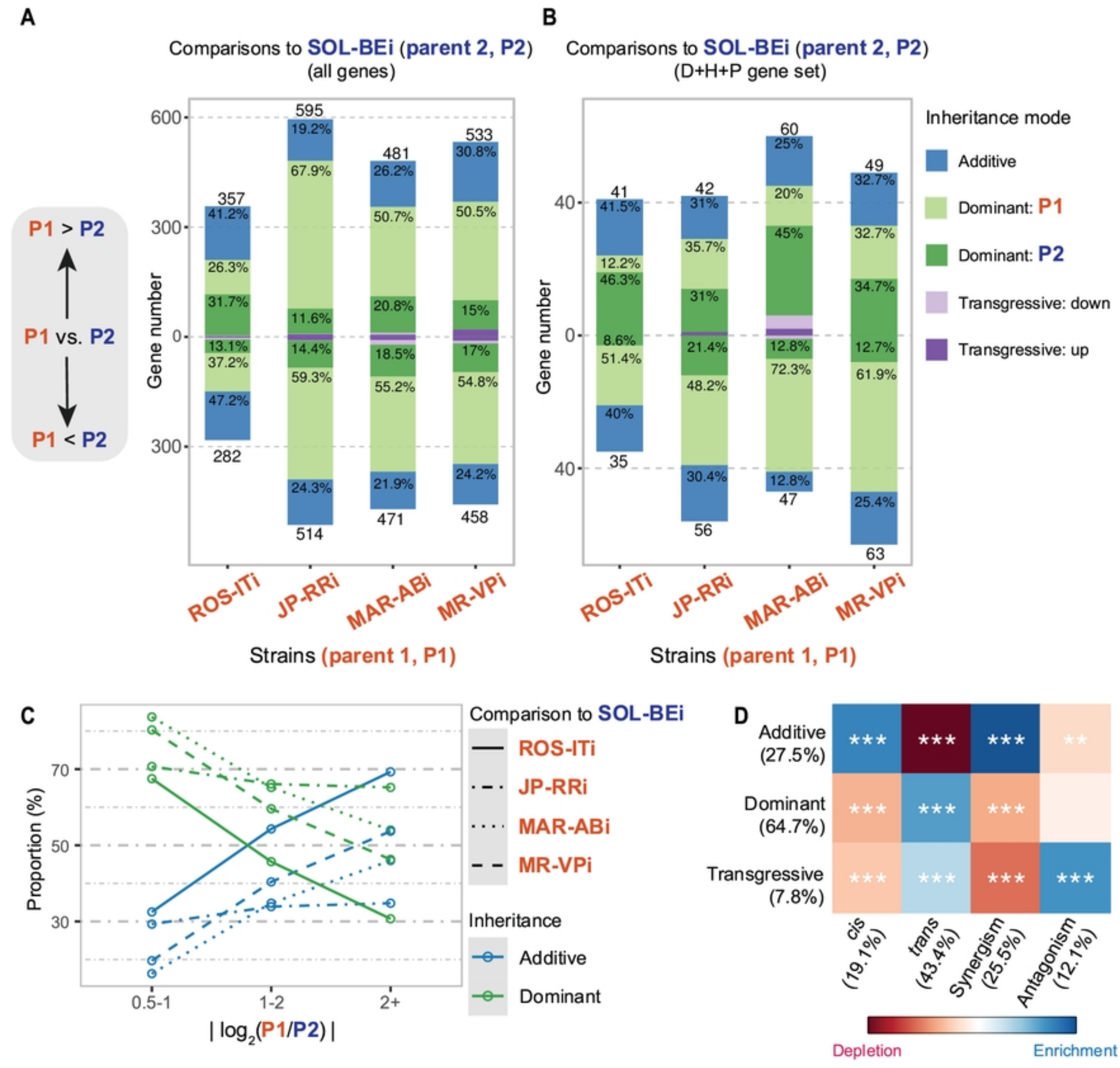
A
Comparisons to SOL-BEi (parent 2, P2)
(all genes)
P1 > P2
P1 vs. P2
P1 < P2
Gene number
600
300
0
300
357
41.2%
26.3%
31.7%
13.1%
37.2%
47.2%
282
595
19.2%
67.9%
11.6%
14.4%
59.3%
24.3%
514
481
26.2%
50.7%
20.8%
18.5%
55.2%
21.9%
471
533
30.8%
50.5%
15%
17%
54.8%
24.2%
458
ROS-ITi
JP-RRi
MAR-ABi
MR-VPi
Strains (parent 1, P1)
B
Comparisons to SOL-BEi (parent 2, P2)
(D+H+P gene set)
Gene number
40
0
40
41
41.5%
12.2%
46.3%
8.6%
51.4%
40%
35
42
31%
35.7%
31%
21.4%
48.2%
30.4%
56
60
25%
20%
45%
12.8%
72.3%
12.8%
47
49
32.7%
32.7%
34.7%
12.7%
61.9%
25.4%
63
ROS-ITi
JP-RRi
MAR-ABi
MR-VPi
Strains (parent 1, P1)
Inheritance mode
Additive
Dominant: P1
Dominant: P2
Transgressive: down
Transgressive: up
C
Proportion (%)
70
50
30
0.5-1
1-2
2+
| log2(P1/P2) |
Comparison to SOL-BEi
ROS-ITi
JP-RRi
MAR-ABi
MR-VPi
Inheritance
Additive
Dominant
D
Additive (27.5%)
Dominant (64.7%)
Transgressive (7.8%)
***
**
cis (19.1%)
trans (43.4%)
Synergism (25.5%)
Antagonism (12.1%)
Depletion
Enrichment

Fig 6